Divergent Functional Properties of Ryanodine Receptor Types 1 and 3 Expressed in a Myogenic Cell Line

James D. Fessenden,* Yaming Wang,† Rennee A. Moore,* S. R. Wayne Chen,‡ Paul D. Allen,† and Isaac N. Pessah*

*Department of Molecular Biosciences, School of Veterinary Medicine, University of California Davis, Davis, California 95616 USA; †Department of Anesthesia Research, Brigham and Women's Hospital, Boston, Massachusetts 02115 USA; and ‡Department of Biochemistry and Molecular Biology, University of Calgary, Alberta, Canada

ABSTRACT Of the three known ryanodine receptor (RyR) isoforms expressed in muscle, RyR1 and RyR2 have well-defined roles in contraction. However, studies on mammalian RyR3 have been difficult because of low expression levels relative to RyR1 or RyR2. Using the herpes simplex virus 1 (HSV-1) helper-free amplicon system, we expressed either RyR1 or RyR3 in 1B5 RyR-deficient myotubes. Western blot analysis revealed that RyR1- or RyR3-transduced cells expressed the appropriate RyR isoform of the correct molecular mass. Although RyR1 channels exhibited the expected unitary conductance for Cs^+ in bilayer lipid membranes, 74 of 88 RyR3 channels exhibited pronounced subconductance behavior. Western blot analysis with an FKBP12/12.6-selective antibody reveals that differences in gating behavior exhibited by RyR1 and RyR3 may be, in part, the result of lower affinity of RyR3 for FKBP12. In calcium imaging studies, RyR1 restored skeletal-type excitation-contraction coupling, whereas RyR3 did not. Although RyR3-expressing myotubes were more sensitive to caffeine than those expressing RyR1, they were much less sensitive to 4-chloro-*m*-cresol (CMC). In RyR1-expressing cells, regenerative calcium oscillations were observed in response to caffeine and CMC but were never seen in RyR3-expressing 1B5 cells. In [^{3}H]ryanodine binding studies, only RyR1 exhibited sensitivity to CMC, but both RyR isoforms responded to caffeine. These functional differences between RyR1 and RyR3 expressed in a mammalian muscle context may reflect differences in association with accessory proteins, especially FKBP12, as well as structural differences in modulator binding sites.

INTRODUCTION

Calcium is a key molecule involved in a wide range of cellular signaling processes. Increases in cytoplasmic calcium levels lead to many diverse cellular responses such as protein secretion, cell motility, and gene activation. A well-characterized role attributed to increases in cytoplasmic calcium is the activation of contraction in striated muscle, where calcium stored in the sarcoplasmic reticulum (SR) is released via the activation of the intracellular calcium release channel, the ryanodine receptor (RyR).

The ryanodine receptor is a large (subunit molecular mass ~565 kDa) homotetrameric protein embedded in the SR membrane. Three RyR isoforms have been discovered, which are encoded by three separate genes (McPherson and Campbell, 1993). RyR1 was initially purified and cloned from skeletal muscle (Pessah et al., 1986; Takeshima et al., 1989), whereas RyR2 was first characterized in cardiac muscle (Inui et al., 1987). RyR3 was first discovered in epithelial cells (Giannini et al., 1992) and brain (Hakamata et al., 1992), where its cDNA was isolated based on homology to the other RyR isoforms.

Both RyR1 and RyR2 play key roles in excitation-contraction (e-c) coupling. In this process, depolarization of the muscle cell is detected by dihydropyridine-sensitive voltage-gated calcium channels (dihydropyridine receptors, DHPRs) in the plasma membrane, which in turn activate the RyRs present in the SR. Subsequent efflux of calcium through the activated RyRs triggers muscle contraction. In contrast, the physiological function of RyR3 is less well understood, even though this isoform has been detected in many tissues, including parotid, spleen, esophagus, and testis (Giannini et al., 1995). RyR3 is often coexpressed with other RyR isoforms, although RyR3 is usually not the predominant isoform. For example, in adult bovine diaphragm, RyR3 constitutes only ~5% of the total [^{3}H]ryanodine binding sites (the remainder being RyR1; Jeyakumar et al., 1998), and in most adult mammalian fast twitch muscle it accounts for only 0–0.2% of the total. An exception to this finding occurs in adult avian, amphibian, and fish skeletal muscle (Airey et al., 1990; Olivares et al., 1991; Lai et al., 1992b), which express approximately equal levels of the α and β RyR isoforms (homologous to the RyR1 and RyR3 isoforms, respectively).

Interestingly, RyR3 levels in many different muscle types often display a distinct developmental profile (Bertocchini et al., 1997), and in skeletal muscle cell lines RyR3 levels increase concomitantly with cellular differentiation (Tarroni et al., 1997). However, the functional consequences of these expression patterns are not known. In neonatal skeletal muscle, tension development in response to the RyR agonist caffeine and contractile force in response to electrical field stimulation are reduced in transgenic RyR3-deficient mice (Bertocchini et al., 1997). However, in skeletal muscle from adult mice lacking RyR3, e-c coupling, calcium-induced calcium release (CICR), and cell contraction are essentially

Received for publication 15 March 2000 and in final form 1 August 2000.

Address reprint requests to Dr. Isaac N. Pessah, Department of Molecular Biosciences, School of Veterinary Medicine, University of California Davis, 1 Shields Ave, Davis, CA 95616. Tel.: 530-752-6696; Fax: 530-752-4698; E-mail: inpessah@ucdavis.edu.

0006-3495/00/11/2509/17 $2.00

normal compared to wild type (Takeshima et al., 1996; Bertocchini et al., 1997; Dietze et al., 1998). Recent work indicates that although the overall level of RyR3 declines during skeletal muscle maturation, the amount of RyR3 in a subset of adult skeletal muscle fibers remains at high levels (Flucher et al., 1999). These results taken together suggest that while the contribution of RyR3 to adult mammalian skeletal muscle function is speculative, RyR3 could have an important accessory role in both neonatal and adult muscle contraction.

Recent functional studies have described [^{3}H]ryanodine binding and single-channel behavior of both native and recombinant RyR3 as well as cellular calcium regulation of recombinant RyR3. This has been done in one of two ways: 1) by either immunoprecipitation with RyR3-selective antibodies (Murayama and Ogawa, 1997; Jeyakumar et al., 1998; Murayama et al., 1999) or biochemical isolation from diaphragm (Sonnleitner et al., 1998), or 2) by transfecting RyR3 cDNA into mammalian nonmuscle cell lines such as HEK293 (Chen et al., 1997) or Chinese hamster ovary cells (Saeki et al., 1998). While this work has provided useful cellular and molecular information concerning RyR3, the lack of a skeletal muscle context used in these studies limits conclusions about its role in skeletal muscle contraction.

We have utilized a new approach, which is to express RyR1 and RyR3 in the RyR-deficient 1B5 myogenic cell line (Moore et al., 1998; Protasi et al., 1998). 1B5 cells can be differentiated into multinucleated myotubes and express the key triadic proteins, including DHPR, 12-kDa FK506 binding protein (FKBP12), calsequestrin, and triadin, but are completely deficient in all RyR isoforms, as judged by ryanodine binding, RyR immunocytochemistry, Western blot analysis, and fluorescence calcium imaging. In this study, we report the divergent physiological and pharmacological properties of RyR1 and RyR3 expressed at comparable levels in 1B5 myotubes, revealing the importance of both molecular structure and cellular context in defining the functional phenotype of these RyR isoforms.

MATERIALS AND METHODS

Cell culture

1B5 cells were cultured in growth medium consisting of Dulbecco's modified Eagle's medium (DMEM) containing 100 units/ml penicillin-G, 100 μg/ml streptomycin sulfate, 2 mM glutamine, and 20% (v/v) fetal bovine serum (Gibco Laboratories, Gaithersburg, MD) at 37°C in 10% CO_2 (Moore et al., 1998). For Fura-2 ratio fluorescence imaging measurements, cells were grown in 20% fetal bovine serum-DMEM in collagen-coated 35-mm or 72-well polystyrene plates (Nalge Nunc International, Rochester, NY). When the cells reached ~50% confluence, they were stimulated to differentiate into multinucleated myotubes by replacing the growth medium with DMEM supplemented with 5% (v/v) heat-inactivated horse serum (Gemini Bio-Products, Calabasas, CA), 2 mM glutamine, and antibiotics as above. The cells were differentiated at 17.5% CO_2, 37°C, for 5–7 days.

C2C12 myoblasts (American Type Culture Collection, Manassas, VA; Yaffe and Saxel, 1977) were cultured and differentiated as described for 1B5 cells (above), except that C2C12 cells were differentiated at 10% CO_2, 37°C, for 5–7 days.

Viral infection

Herpes simplex virus 1 (HSV-1) virions containing the cDNA encoding either RyR1 or RyR3 were prepared as described previously (Wang et al., 2000). 1B5 cells differentiated for 5 days were infected with RyR cDNA-containing helper-free HSV-1 amplicon virions in the presence of antibiotic-free 5% heat-inactivated horse serum at 17.5% CO_2, 37°C, at 1×10^5 infectious units (IU)/ml after the initial optimization studies were done (see Results). After 24 h, the virus-containing medium was replaced with standard differentiation media, and the infected myotubes were incubated as above for an additional 24 h. These myotubes were then either examined for calcium responses or fixed for immunohistochemical analysis (see below).

Immunohistochemistry

Differentiated 1B5 myotubes were fixed in cold methanol (−20°C) for 15 min and washed with phosphate-buffered saline (PBS) (Gibco Laboratories). Cells were then permeabilized with PBS/0.05% Tween-20 for 1 min before blocking with PBS/5% normal goat serum three times for 10 min each. Blocking buffer was removed, and anti-RyR1/3 34C monoclonal antibody (Developmental Studies Hybridoma Bank, University of Iowa, Iowa City, IA; Airey et al., 1990) was applied at a concentration of 1:25 in PBS for 1 h at 25°C. Cells were washed with PBS/5% normal goat serum three times and then incubated with Cy-3-conjugated goat anti-mouse IgG (1:1000) (Jackson ImmunoResearch Laboratories, West Grive, PA) for 1 h. The cells were then rinsed three times with PBS and mounted with Gel/Mount (Biomeda Corp., Foster City, CA). Cy-3 fluorescence was visualized with a Nikon Diaphot microscope (Nikon, Melville, NY) with an epifluorescence attachment (510–560 nm excitation, 590 nm emission).

Cell counts

The intracellular distribution of RyR immunolabeling was determined by examining randomly selected fields from RyR1-infected 1B5 myotubes, using a 20× lens. Immunolabeled cells were categorized as exhibiting "reticular," "punctate," or "mixed" type immunoreactivity, as defined in the companion report (Protasi et al., 2000). The relative percentage of cells displaying these labeling patterns was determined from four 20× fields from three RyR1-infected 35-mm dishes at two different viral concentrations (1 and 2×10^5 IU/ml).

Calcium imaging

Differentiated 1B5 myotubes were loaded with the calcium indicator dye Fura-2 at 37°C, for 20 min in "imaging buffer" (125 mM NaCl, 5 mM KCl, 2 mM KH_2PO_4, 2 mM $CaCl_2$, 1.2 mM $MgSO_4$, 6 mM glucose, and 25 mM HEPES, pH 7.4) supplemented with 0.05% bovine serum albumin (fraction V) and 5 μM Fura-2/AM (Molecular Probes, Eugene, OR). The cells were then washed three times with 1 ml imaging buffer supplemented with 250 μM sulfinpyrazone. The cells were transferred to a Nikon Diaphot microscope and Fura-2 was excited alternately at 340 nm and 380 nm, using a DeltaRam fluorescence imaging system (Photon Technology International, Princeton, NJ). Fluorescence emission was measured at 510 nm with a 10× quartz objective. Data were collected with an IC-300 intensified CCD camera (Photon Technology International) from regions consisting of 20–100 individual cells. Image files representing raw fluorescence data were saved to a hard drive and subsequently analyzed using Imagemaster software (Photon Technology International). Data presented as the ratio of

the 510-nm emissions of Fura-2 obtained at 340- and 380-nm excitation (ratio 340/380) was collected from individual cells.

RyR agonists were dissolved in imaging buffer, and 10 volumes (100 μl) was perfused into microtiter wells containing RyR-infected 1B5 myotubes. Electrical field stimulation was accomplished using bipolar solid-state silver electrodes connected to a Pulsar 4i stimulator (Frederick Haer and Co., Bowdoinham, ME). The electrodes were placed at the edges of the field of cells being imaged, and 5-V, 200-ms pulses with a 20-s interpulse interval were applied.

Membrane preparations

Myotubes infected with RyR cDNA-containing viruses were rinsed two times with ice-cold PBS and scraped from 100-mm plates in the presence of 3 ml harvest buffer (137 mM NaCl, 3 mM KCl, 8 mM Na_2HPO_4, 1.5 mM KH_2PO_4, 1.5 mM EDTA, pH 7.4). Cells were centrifuged for 5 min at 100 $\times$ *g*, and each cell pellet was resuspended in ice-cold hypotonic lysis buffer (1 mM EDTA, 1 μM leupeptin, 250 μM phenylmethylsulfonyl fluoride, 10 μg/ml pepstatin A, 10 μg/ml aprotinin, 10 mM HEPES, pH 7.4). The resuspended pellet was homogenized on ice using a PowerGen 700D, for 3 $\times$ 5 s at 1400 rpm (Fisher Scientific, Pittsburgh, PA). An equal volume of ice-cold 20% sucrose buffer (10 mM HEPES, pH 7.4) was added, and the tissue was further homogenized as above. This homogenate was centrifuged at 110,000 $\times$ *g* in a Beckman Ti80 rotor (Palo Alto, CA) for 1 h at 4°C. The pellet was then resuspended in 4 ml of buffer containing 10% sucrose and 10 mM HEPES (pH 7.4). The resuspended pellet was divided into small aliquots, frozen in liquid nitrogen, and stored at −80°C until it was used for binding analysis. For Western blot analysis and single-channel measurements, the membranes were further purified by sedimentation of the crude membranes at 40,000 $\times$ *g* on a sucrose gradient consisting of layers of 10%, 27%, and 45% (w/w) sucrose and 10 mM HEPES (pH 7.4). The 27–45% interface containing heavy SR membranes was isolated from the gradient, diluted in 10 mM HEPES (pH 7.4), and pelleted at 110,000 $\times$ *g* for 1 h. The pellet was resuspended in 10% sucrose, 10 mM HEPES (pH 7.4); divided into small aliquots; and stored at −80°C.

Membranes enriched in markers of junctional SR were prepared from rabbit fast skeletal muscle, using the method of Saito and co-workers (Saito et al., 1984) in the presence of 100 μM phenylmethylsulfonyl fluoride and 10 μg/ml leupeptin. Purified heavy SR from the 38–45% interface of sucrose density gradients was pelleted, resuspended at 2–6 mg/ml (Lowry et al., 1951), frozen in liquid nitrogen, and stored at −80°C until needed. Membranes enriched in cardiac junctional SR were prepared from rabbit heart, using the method of Feher and co-workers (Feher and Davis, 1991). Avian junctional SR membranes were isolated from avian pectoralis muscle according to the method of Airey and co-workers (Airey et al., 1990).

Western blot analysis

The methods used for gel electrophoresis and Western blot analysis were described in detail elsewhere (Moore et al., 1998). Briefly, proteins were denatured at 100°C for 30 min in reducing sample buffer, which consisted of 48 mM NaH_2PO_4, 170 mM Na_2HPO_4, 0.02% bromophenol blue, 1% sodium dodecyl sulfate, and 5% β-mercaptoethanol (pH 7.4). Protein (0.5–20 μg) was loaded onto 5% sodium dodecyl sulfate-polyacrylamide gels and electrophoresed at constant voltage (200 V). The size-separated proteins were transferred onto polyvinylidene difluoride microporous membranes (Millipore, Bedford, MA), using an electroblotter (Mini Trans-Blot; Bio-Rad Laboratories, Hercules, CA) overnight at 30 V (4°C) and for 1 h at 200 V. Polyvinylidene difluoride transfers were incubated for 1 h at 25°C in TTBS (137 mM NaCl, 20 mM Tris-HCl, 0.05% Tween 20, pH 7.6) containing 5% (w/v) nonfat milk. The blots were then probed with either a primary antibody that recognizes both RyR1 and RyR3 (34C: 1:200 dilution), a RyR2-specific (C3–33: 1:250 dilution, generously provided by G. Meissner; Lai et al., 1992a) or RyR3-specific (Ab 7165: 1:1000 dilution, generously provided by Dr. G. Meissner; Protasi et al., 2000) antibody. Immunophilins FKBP12 and FKBP12.6 were detected using selective polyclonal antibody PA1–026 (Affinity Bio-Reagents, Golden, CO). The selected antibody was diluted in TTBS plus 1% bovine serum albumin and incubated with the blot for 1 h at 25°C. The immunoblots were rinsed three times with TTBS and then incubated either with a horseradish peroxidase-conjugated sheep anti-mouse IgG (1:20,000) (for blots probed with 34C or C3–33) or goat anti-rabbit IgG (1:10,000) (for blots probed with Ab 7165 and PA1–026) (Sigma Chemical Co., St. Louis, MO) for 1 h. After a final rinse step with TTBS, enhanced chemiluminescence techniques (NEN Life Science Products, Boston, MA) were used to visualize the immunoblots.

Radioligand binding assay

High-affinity equilibrium binding of [^{3}H]ryanodine (62 Ci/mmol; New England Nuclear, Boston, MA) to membrane homogenates prepared from differentiated 1B5 myotubes was performed in the presence of 140–250 mM KCl, 15 mM NaCl, 10% sucrose, 20 mM HEPES (pH 7.1), 1 μM Ca^{2+}, and 10 nM [^{3}H]ryanodine. The binding reaction was conducted at 37°C for 3 h in 0.5 ml containing 50 μg of whole membrane homogenate prepared from 1B5 cells. Nonspecific binding was assessed in the presence 10 μM unlabeled ryanodine. Pharmacological responses to 4-chloro-*m*-cresol (CMC) (50–500 μM) and caffeine (200 μM to 40 mM) were examined in the presence of 10 nM [^{3}H]ryanodine and 1 μM Ca^{2+}. Separation of bound and free ligand was performed by rapid filtration through Whatman GF/B glass fiber filters, using a Brandel (Gaithersburg, MD) cell harvester. Filters were washed with 2 volumes of 5 ml ice-cold wash buffer containing 20 mM Tris-HCl, 250 mM KCl, 15 mM NaCl, 50 μM $CaCl_2$ (pH 7.1) and placed in vials with 5 ml scintillation cocktail (Ready Safe; Beckman Instruments, Fullerton, CA). The [^{3}H]ryanodine remaining on the filters was quantified by liquid scintillation spectrometry.

Single-channel measurements

Heavy SR membrane vesicles isolated from RyR1- or RyR3-infected 1B5 cells were fused into a bilayer lipid membrane (BLM) made from a 5:2 mixture of synthetic phosphatidylethanolamine and phosphatidylcholine suspended at 50 mg/ml in decane. The BLM was formed across a 200–250-μm hole in a polystyrene cup separating two chambers (*cis* and *trans*) of 0.7 ml each. Microsomal membrane vesicles (0.1–5 μg protein) were added to the *cis* chamber in the presence of 200 μM Ca^{2+}. The *cis* and *trans* chambers contained 500 mM CsCl (or CH_3O_3SCs), 20 mM HEPES (pH 7.4) and 100 mM CsCl (or CH_3O_3SCs), 20 mM HEPES (pH 7.4), respectively. After fusion, 300 μM EGTA was added to the *cis* chamber to prevent any additional fusion events. The *cis* chamber was then perfused with a solution composed of 500 mM CsCl (or CH_3O_3SCs) and 20 mM HEPES (pH 7.4) (asymmetrical conditions, 5:1 *cis:trans*; or symmetrical conditions, 1:1). Single-channel current was measured under voltage clamp, using a Dagan 3900 amplifier (Dagan Instruments, Minneapolis, MN). Holding potentials were with respect to the *trans* (ground) chamber, and positive current was defined as current flowing from *cis* to *trans*. Current signals were captured at 10 kHz and filtered at 1 or 2 kHz, using a four-pole Bessel filter. Data were digitized with a Digidata 1200 interface (Axon Instruments, Burlingame, CA) and stored on computer for subsequent analysis.

Experimental reagents were added to the *cis* chamber and stirred for 30 s. Subsequent channel gating behavior was recorded for 1–20 min, using Axotape software (Axon Instruments). Single-channel data from BLM experiments were analyzed using pCLAMP software (pCLAMP version 7.0; Axon Instruments), and figures were prepared using Origin 5.0 (Microcal, Northampton, MA).

RESULTS

Expression of RyR1 and RyR3 protein in differentiated 1B5 myotubes

Expression of RyR protein in 1B5 myotubes was achieved using HSV-1 virions that contain the cDNA for either rabbit RyR1 or RyR3. Increasing amounts of RyR1 cDNA-containing viral particles resulted in a linear increase in the number of RyR immunoreactive 1B5 cells. At the highest level of virus tested (4×10^5 infectious units/ml), $56 \pm 9\%$ of the 1B5 cells in randomly selected 20× microscopic fields expressed RyR1 protein. At an equivalent level of infection, RyR3 cDNA-containing viruses gave essentially the same transfection efficiency as viruses containing RyR1 cDNA.

In agreement with our published results (Moore et al., 1998), no expression of RyRs was detected by Western blot in untransfected 1B5 myotubes probed with antisera to RyR1/RyR3 (34C monoclonal; Fig. 1 *A*, *lane 2*), RyR2 (C3–33 monoclonal; data not shown), or RyR3 alone (polyclonal Ab 7165; Fig. 1 *B, lane 4*). Western blot analysis of heavy SR membranes isolated from RyR1- or RyR3-infected 1B5 myotubes revealed each to possess a single high-molecular-weight protein when probed with 34C, a monoclonal antibody that recognizes both RyR1 and RyR3 (Fig. 1 *A*). RyR3 (*lane 4*) migrated slightly ahead of RyR1 (*lane 3*), which is in agreement with the lower molecular weight of RyR3 deduced from its cDNA sequence. The migration of RyR1 and RyR3 isolated from 1B5 cells was similar to the migration of RyR1 from rabbit junctional sarcoplasmic reticulum (JSR; Fig. 1 *A, lane 1*) and RyR3 from avian skeletal muscle (Fig. 1 *B, lane 1*), respectively. In addition, a mixture from separate preparations of either RyR1- or RyR3-infected 1B5 myotubes yielded a doublet on the Western blot (Fig. 1 *A, lane 5*), thus confirming that the difference in migration of RyR1 and RyR3 reflected actual differences in protein apparent molecular mass rather than possible electrophoretic artifacts. Finally, the RyR3-selective antibody (Fig. 1 *B*) detected protein from RyR3- (*lane 2*) but not RyR1- (*lane 3*) infected 1B5 myotubes or from rabbit skeletal muscle JSR (*lane 5*). The RyR2-selective antibody (C3–33) did not detect protein from either RyR1- or RyR3-infected myotubes (data not shown).

Reconstitution of functional RyR responses

Single-channel studies

Further studies were performed with heavy SR membranes isolated from 1B5 myotubes fused in a BLM to study the

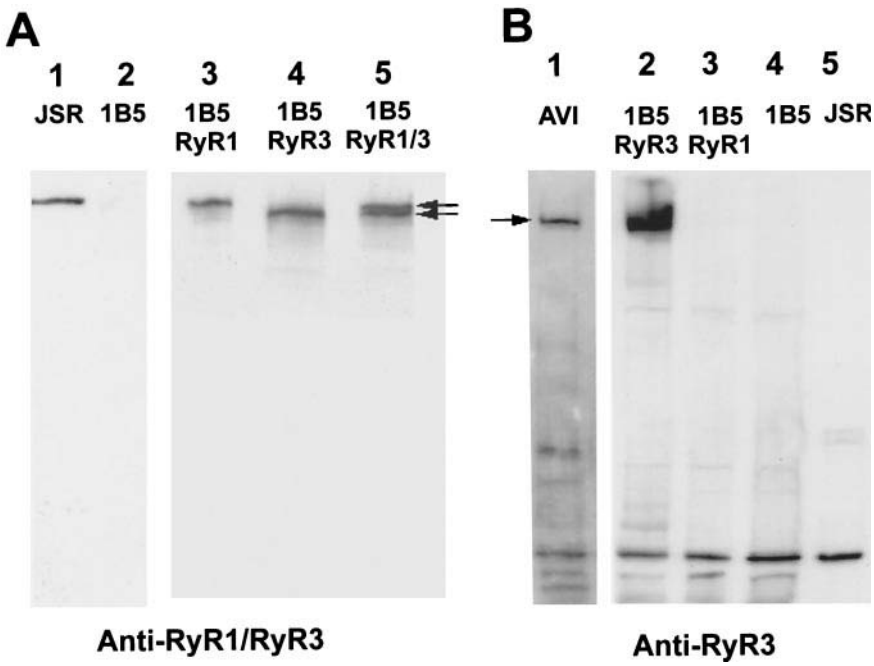

FIGURE 1 Viral transduction of RyR1 or RyR3 cDNAs yields full-length protein in 1B5 myotubes. (*A*) RyR immunoreactivity was detected using an anti-RyR1/RyR3 antibody (34C) and visualized using enhanced chemiluminescence as described in Materials and Methods. Lanes were loaded as follows: *Lane 1*: Rabbit skeletal muscle JSR (1 μg). *Lane 2*: Control (noninfected) 1B5 cells (20 μg). *Lane 3*: RyR1-infected 1B5 cells (20 μg). *Lane 4*: RyR3-infected 1B5 cells (20 μg). *Lane 5*: Mixture of extracts prepared from RyR1- and RyR3-infected 1B5 cells (20 μg each). Arrows indicate the presence of the doublet in lane 5 (RyR1, *top*; RyR3, *bottom band*). Film was exposed for 10 s for lanes 3–5 and for 3 min for lanes 1 and 2. (*B*) RyR immunoreactivity was detected using an anti-RyR3 polyclonal antibody (7165). *Lane 1*: Avian skeletal muscle JSR (2 μg). *Lane 2*: RyR3-infected 1B5 cells (20 μg). *Lane 3*: RyR1-infected 1B5 cells (20 μg). *Lane 4*: Control (noninfected) 1B5 cells (20 μg). *Lane 5*: Rabbit skeletal muscle JSR (2 μg). Film was exposed for 3 min for lane 1 and for 30 s for lanes 2–5. The arrow indicates the position of the RyR3 band in avian skeletal muscle JSR. Note: Increasing the exposure time to 10 min did not reveal any RyR bands in lanes 3–5.

gating behavior of virally transduced RyR1 and RyR3 channels. Of $n = 60$ successful channel fusions, virally transduced recombinant RyR1 exhibited rapid gating kinetics with a single unitary cesium conductance ranging from 407 to 485 pS. The pharmacological responses of expressed RyR1 were indistinguishable from those measured from rabbit skeletal muscle SR. These results are in agreement with previous findings from experiments using lipofectamine to introduce RyR1 cDNA into 1B5 myotubes (Moore et al., 1998) and subsequent results for viral infection (Wang et al., 2000). In contrast, RyR3 channels exhibited stable and frequent transitions to and from subconductance levels that were most evident at suboptimal (5–10 μM) *cis* Ca^{2+}. Fig. 2 *A* shows a representative RyR3 channel illustrating regular gating transitions from full closed to ¼ state and then ¼ to full open. Gating transitions to ½ and ¾ conductances were also evident in most traces, although they are somewhat less frequent (Fig. 2 *A*, *inset showing all-points histogram*). Subconductance behavior of RyR3 reconstituted from 1B5 SR membranes was seen in

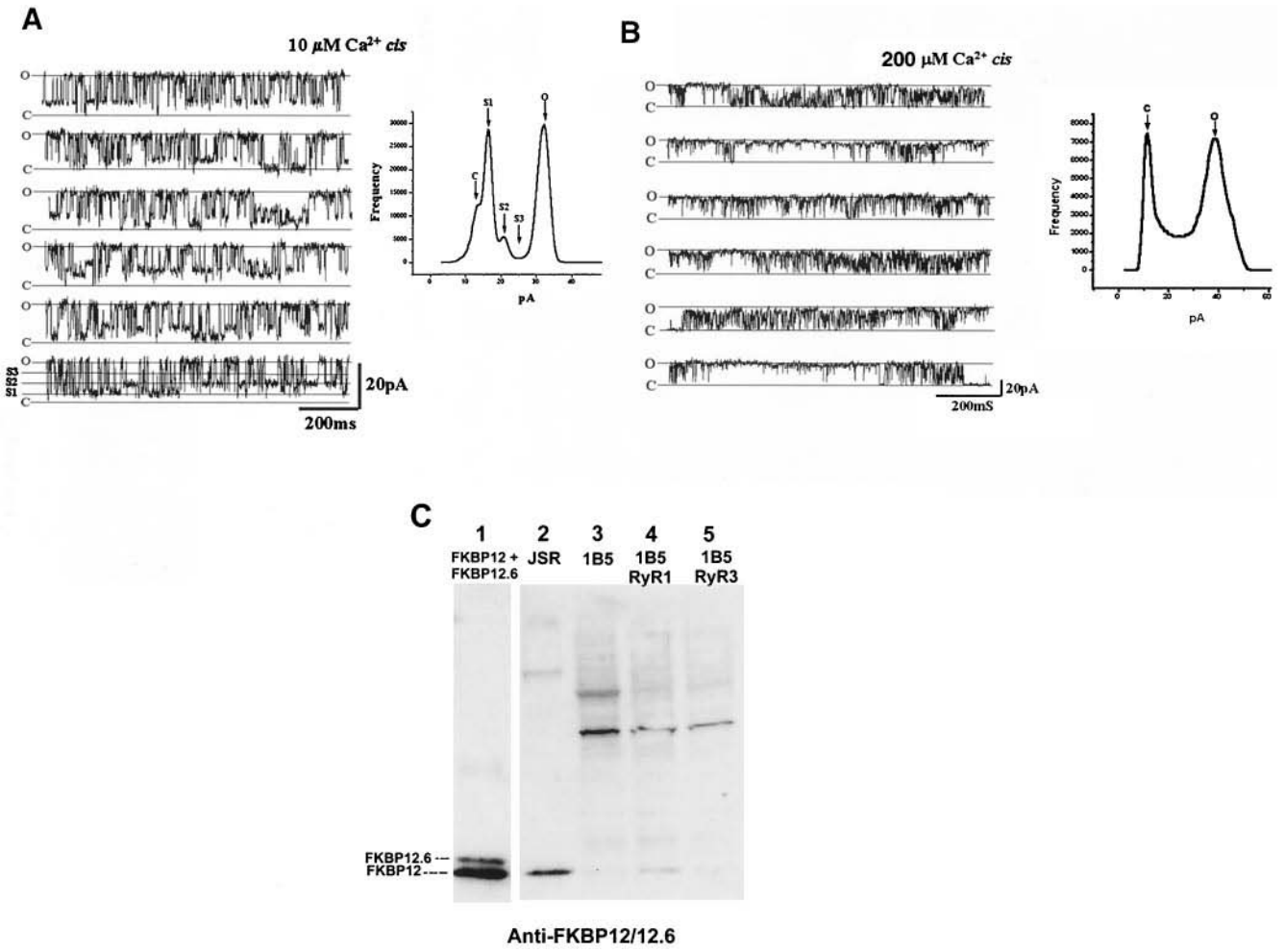

FIGURE 2 Sarcoplasmic reticulum enriched in RyR3 exhibits pronounced subconductance behavior when reconstituted in lipid bilayers. (*A*) Stable subconductance transitions were apparent (long-lived) when *cis* Ca^{2+} was 5–10 μM and the open probability (P_o) was low. This type of gating was observed in 84% of $n = 88$ RyR3 channels reconstituted and was never seen with transgenic RyR1 channels ($n = 60$ reconstitutions) isolated from 1B5 myotubes that possessed only the 456 ± 32 pS transition. *Inset*: All-points histogram of channel trace in *A*, indicating the relative frequencies of the closed state (C), the subconductance states (S1, S2, and S3), and the full open state (O). (*B*) RyR3 channel where the *cis* [Ca^{2+}] was elevated to 200 μM. The frequency and lifetime of full 480-pS open-state transitions was increased, although subconductances were still apparent in the trace and all-points histograms (*inset*). See text for details. The holding potential was +20 mV, with 5:1 *cis*:*trans* Cs^+ as the current carrier. (*C*) FKBP12 is enriched in heavy SR membranes isolated from RyR1-expressing but not RyR3-expressing 1B5 myotubes. Polyclonal antibody PA1-026 selectively recognized human recombinant FKBP12 and FKBP12.6 (*lane 1*; 10 ng each). Isolated junctional SR from rabbit skeletal muscle contained only FKBP12 (*lane 2*; 3 μg protein). Likewise, the heavy SR fractions from null 1B5 myotubes were found to contain a low level of FKBP12 (*lane 3*; 20 μg protein). Transduction of 1B5 myotubes with RyR1 cDNA resulted in a significant increase in immunoreactive FKBP12 protein in the same heavy SR fraction enriched in RyR1 protein (*lane 4*; 20 μg protein). In contrast, SR obtained from RyR3-infected 1B5 myotubes (*lane 5*, 20 μg protein) showed levels of FKBP12 similar to those of SR isolated from null myotubes. These results were repeated four times with the same results.

$n = 74$ of 88 channels reconstituted in the BLM. The remaining 16% ($n = 14$) of RyR3 channels showed little or no subconductance behavior. In channels exhibiting multiple conductance states, the incidence of subconductance transitions decreased in the presence of optimal (50–200 μM) *cis* Ca^{2+}, and the full open (480 pS) and full closed transitions predominated (Fig. 2 *B*). The RyR3 channels maintained their expected sensitivity to ryanodine and ruthenium red, which stabilized a long-lived ½ conductance and fully blocked the channel, respectively (data not shown).

The major T-cell immunophilin FKBP12 has been shown to tightly bind RyR1 and to colocalize with the channel complex in isolated SR (Marks, 1996). Heavy SR membranes from null 1B5 myotubes and myotubes transduced with RyR1 or RyR3 cDNA were probed for their ability to bind an anti-FKBP12 polyclonal antibody (Fig. 2 *C*). This antibody recognized both human recombinant FKBP12 and FKBP12.6 (*lane 1*) and FKBP12 associated with junctional SR isolated from rabbit skeletal muscle (*lane 2*). FKBP12 but not FKBP12.6 was detected in SR from null 1B5 myotubes (*lane 3*). The amount of FKBP12 that sedimented with the heavy SR fraction was significantly higher in preparations from cells transduced with RyR1 compared with those transduced with RyR3 (compare *lanes 4* and *5*). These results indicate that FKBP12 may be less tightly associated with RyR3 than with RyR1 and dissociates more readily from the SR fraction during isolation.

Correlation between immunolabeling and recovery of RyR function

Using 1B5 cells grown in microtiter plates, it was possible to directly correlate the recovery of functional responses with RyR immunoreactivity in individual cells (Fig. 3). When resting RyR1-infected 1B5 cells loaded with Fura-2 (Fig. 3 *A*) were stimulated with the RyR agonist 4-chloro-*m*-cresol (500 μM; Fig. 3 *B*), the cytosolic ratio of Fura-2 fluorescence (F340/F380) rapidly increased (Fig. 3 *D*), indicating an elevation in intracellular calcium. Only those

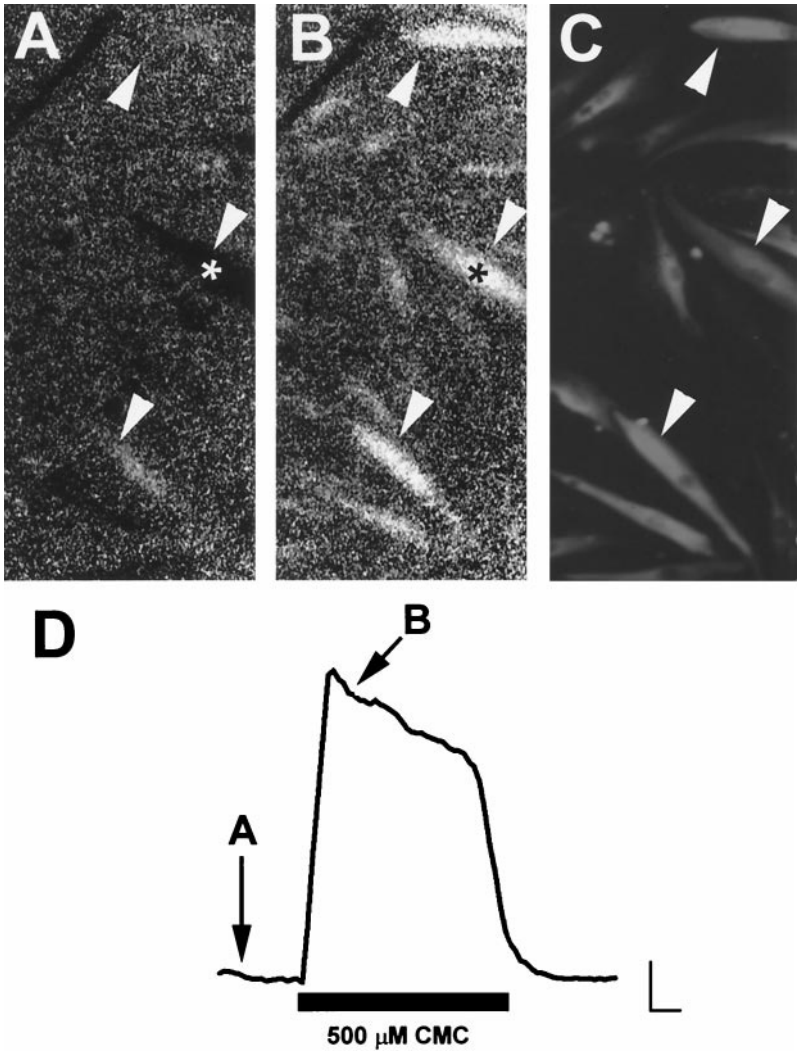

FIGURE 3 Only 1B5 myotubes expressing RyR protein display functional RyR-dependent calcium responses. 1B5 cells grown in collagen-coated 72-well microtiter plates (Terasaki format) were infected with RyR1 cDNA containing pHSV virions at 2×10^5 IU/ml. Cells were examined for calcium responses using Fura-2 as described in Materials and Methods and then fixed and probed for RyR immunoreactivity, using 34C primary antibody. (*A*) F340/F380 ratio of unstimulated 1B5 cells loaded with Fura-2. (*B*) Cells in *A* stimulated with 500 μM 4-chloro-*m*-cresol (CMC). Note: An increase in the brightness of the cells in *B* indicates an increase in F340/F380 ratio of Fura-2. (*C*) The field in *A* and *B*, immunostained with 34C anti-RyR antibody. Note that cells that are immunopositive for RyR expression also respond to CMC in *B*. Each arrowhead in *A–C* indicates the same cell in all three panels. (*D*) Calcium trace of the cell indicated by the asterisk in *A* and *B*. The arrows on the trace indicate the point in the experiment from which the images in *A* and *B* were taken. Calibration bar: 0.1 340/380 ratio units versus 10 s.

cells that exhibited RyR1 immunoreactivity (Fig. 3 *C*) were responsive to CMC. In agreement with previous results (Moore et al., 1998), neither RyR immunoreactivity nor functional responses to RyR agonists were ever observed in uninfected 1B5 cells.

Excitation-contraction coupling

Restoration of "skeletal type" e-c coupling was accomplished by expressing RyR1 but not RyR3 cDNA in 1B5 myotubes. Myotubes expressing RyR1 protein exhibited calcium transients in response to direct electrical field stimulation (5 V, 200 ms), chemical depolarization with 40 mM KCl, or addition of 40 mM caffeine (Fig. 4 *A*). The transduction efficiency of RyR1 cDNA was estimated based on recovery of function by determining the percentage of the total number of Fura-2-loaded cells that responded to 40 mM caffeine. The average responsiveness of RyR1-infected 1B5 myotubes (n = 183 cells tested) to 40 mM caffeine was 45 ± 7% (Fig. 4 *B*). Of these caffeine-responsive cells, 78 ± 7% responded to 40 mM KCl and 18 ± 11% responded to electrical field stimulation. In contrast, although 36 ± 8% of cells infected with RyR3 cDNA-containing virus responded to caffeine (Fig. 4, *C–D*), none of the cells responded to either electrical or chemical depolarization (0 cells of 187 RyR3-expressing cells).

The percentage of RyR1-expressing 1B5 cells that responded to the two different modes of depolarization (KCl

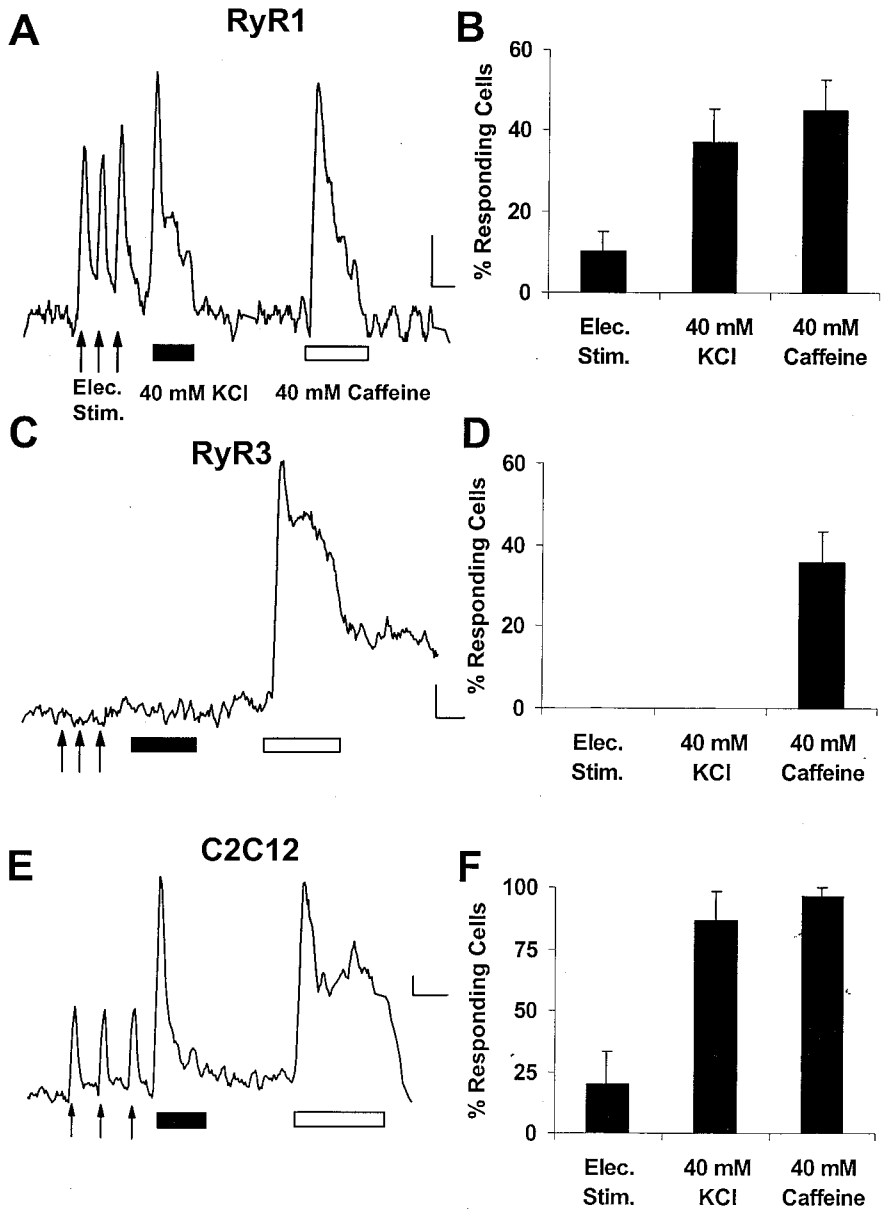

FIGURE 4 Excitation-contraction coupling can be reconstituted in RyR1-expressing but not in RyR3-expressing 1B5 myotubes. 1B5 myotubes infected with either RyR1 (*A*) or RyR3 (*C*) cDNA-containing viruses (1×10^5 IU/ml) or C2C12 myotubes (*E*) were imaged for calcium as described in Materials and Methods. Cells stimulated with three consecutive 5-V, 200-ms pulses spaced 20 s apart (*arrows*) were then depolarized for 30 s, using 40 mM KCl (*filled bar*), and, after washout, stimulated with 40 mM caffeine for 30 s (*unfilled bar*). Finally, cells were treated with 2 μM ionomycin (not shown) to obtain the total number of Fura-2-loaded cells. *B*, *D*, and *F* summarize calcium responses seen in RyR1-expressing 1B5 cells (n = 86 cells), RyR3-expressing 1B5 cells (n = 49 cells), and C2C12 cells (n = 156), respectively. Note: % Responding cells indicates the percentage of cells responding to an agonist relative to the total number of Fura-2-loaded cells. Values represent the mean ± SD from five determinations. Calibration bar for each trace: 0.05 340/380 ratio units versus 25 s.

and field stimulation) were quite different. The reason for this difference was explored using C2C12 cells (Fig. 4, *E–F*), which are derived directly from embryonic mouse skeletal muscle (Yaffe and Saxel, 1977) and thus target RyRs efficiently to calcium release units (CRUs). Similar to RyR1-expressing 1B5 cells, C2C12 cells responded to both electrical and chemical depolarization. Of the total number of Fura-2-loaded cells, 96 ± 4% responded to 40 mM caffeine, and of these cells, 87 ± 11% responded to 40 mM KCl and 20 ± 13% responded to electrical field stimulation. The percentage of cells responding to electrical field simulation was similar between RyR1-expresssing 1B5 cells and C2C12 cells (18 ± 11% and 20 ± 13%, respectively) and was low compared to chemical depolarization with KCl (78 ± 7% and 87 ± 11%, respectively). Therefore, the modest level of responsiveness to electrical field stimulation reflects the relatively low efficiency of this method in depolarizing myotubes rather than improper intracellular targeting of RyR1.

The e-c coupling observed in RyR1-expressing 1B5 cells, like that in C2C12 myotubes was "skeletal type," inasmuch as responses to electrical depolarization were independent of extracellular calcium. Fig. 5 shows a representative RyR1-transduced 1B5 myotube (Fig. 5 *A*) and C2C12 myotube (Fig. 5 *B*), which responded to electrical field stimulation both in the presence of 2 mM extracellular calcium and in nominally calcium-free medium supplemented with 2 mM EGTA (free $[Ca^{2+}] < 10$ nM).

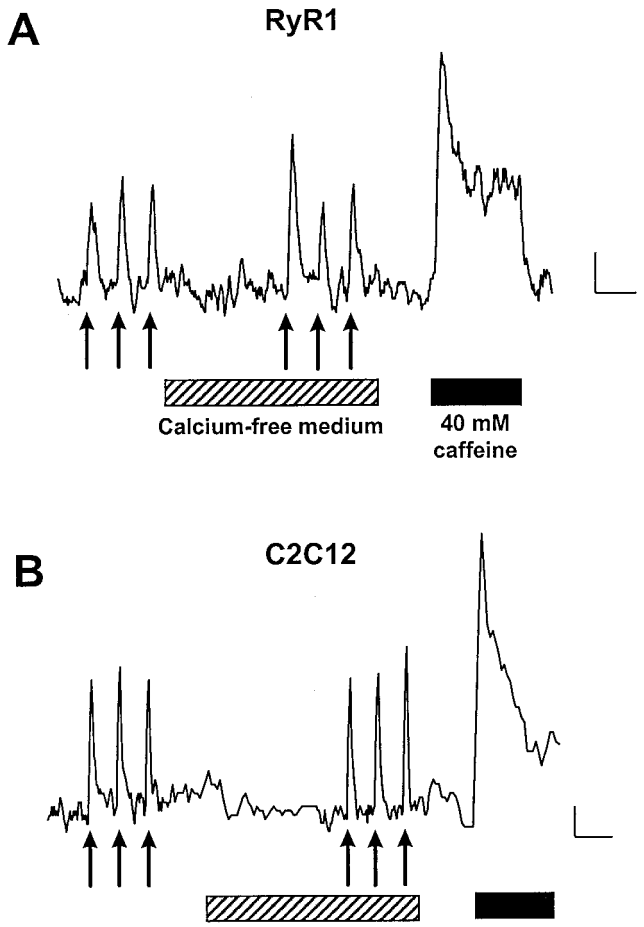

FIGURE 5 Recovery of "skeletal-type" e-c coupling in RyR1-expressing 1B5 myotubes. 1B5 myotubes infected with viruses containing RyR1 cDNA (1×10^5 IU/ml) or C2C12 myotubes were imaged for calcium as described in Materials and Methods. A representative traces from a RyR1-transduced 1B5 myotube and a C2C12 myotube are shown in *A* and *B*, respectively. The myotubes were stimulated with three consecutive electrical pulses (*arrows*) as described in Fig. 4. After a 1-min incubation period in nominally calcium-free imaging buffer supplemented with 2 mM EGTA (*stippled bar*), cells were challenged again with electrical pulses and then with 40 mM caffeine (*filled bar*). Calibration bar: 0.05 340/380 ratio units versus 25 s.

Correlation between RyR1 localization and restoration of e-c coupling

As described (Protasi et al., 2000), 1B5 cells expressing either RyR1 or RyR3 give rise to three patterns of immunolabeling, "punctate," "reticular," and "mixed." Punctate labeling indicates RyRs properly localized to CRUs in the junctional SR membrane in well-differentiated 1B5 myotubes, whereas reticular labeling represents RyRs that have not been targeted to junctions and presumably are localized within the SR/ER lumen. Cells with mixed-type labeling contain both reticular and punctate labeling patterns. The percentage of 1B5 cells expressing RyR1 that contained punctate or mixed RyR1 immunoreactivity was closely correlated with the percentage of cells that responded to chemical depolarization with 40 mM KCl. In calcium imaging studies, as the viral concentration was increased from 1×10^5 to 2×10^5 IU/ml, the number of transduced cells increased from 47% to 69%. However, the percentage of RyR1-expressing cells exhibiting e-c coupling decreased from 78.4% to 50%. In an independent set of parallel experiments, the immunocytochemical labeling patterns of RyR1 were examined. These studies revealed that the percentage of transduced cells with punctate or mixed RyR1 immunoreactivity decreased from 69% to 48% of the total number of immunoreactive cells as the viral titer was increased from 1×10^5 to 2×10^5 IU/ml. Thus the lower viral titer was used for all of the remaining studies to optimize the percentage of cells with proper intracellular targeting of the expressed RyRs.

RyR1 and RyR3 pharmacology

Ryanodine sensitivity

RyR1 or RyR3 expressed in 1B5 myotubes restored ryanodine-induced calcium release (Fig. 6). The effect of 200 μM ryanodine added to individual myotubes expressing transduced RyRs was to gradually raise intracellular Ca^{2+} over several minutes (Fig. 6, *A* and *B*). These effects were

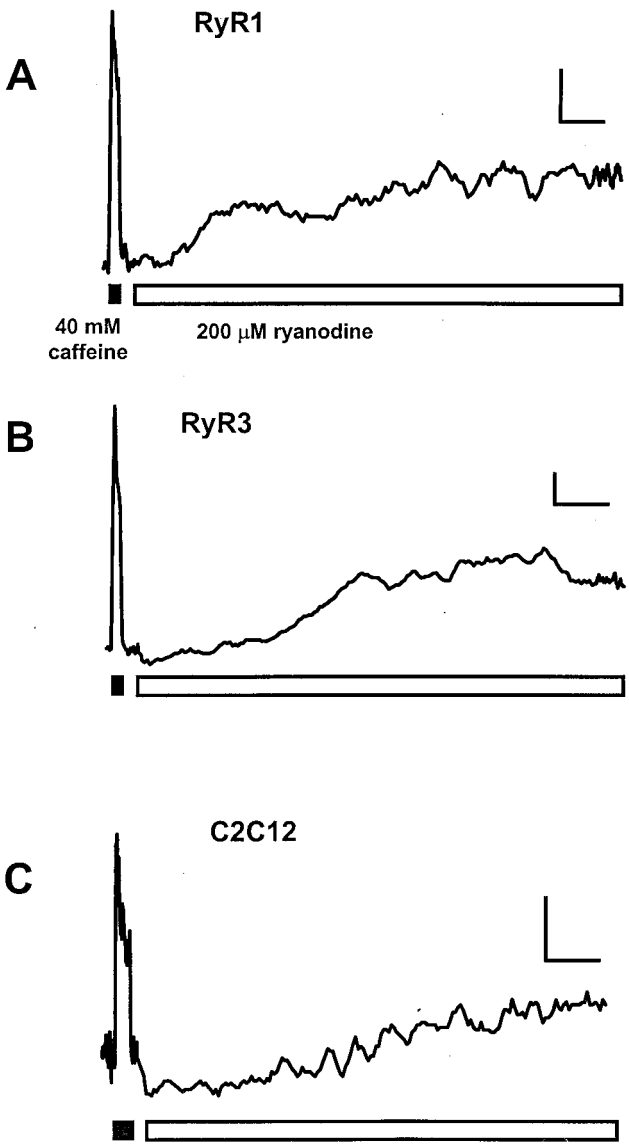

FIGURE 6 RyR1- and RyR3-expressing 1B5 myotubes respond to ryanodine. Cells were cultured and imaged for calcium as described in Materials and Methods. 1B5 cells expressing either RyR1 (*A*) or RyR3 (*B*) as well as C2C12 myotubes (*C*) were challenged with 40 mM caffeine (*black bar*) followed (after washout) by a 30-min exposure to 200 μM ryanodine (*empty bar*). In all three cases, ryanodine exposure resulted in a slow increase in the level of intracellular calcium. Calibration bar: 0.1 340/380 ratio units versus 200 s.

indistinguishable from the actions of ryanodine on C2C12 myotubes (Fig. 6 *C*).

Caffeine sensitivity

The caffeine sensitivity of C2C12 cells and 1B5 cells expressing either RyR1 or RyR3 was determined using calcium imaging of individual myotubes. The dose-response relationship for caffeine was very steep in any given myotube because of a strong component of CICR. Furthermore, in C2C12 cells, or in 1B5 cells expressing RyR1 or RyR3, the magnitude of the calcium increase at threshold caffeine levels was similar to responses seen at maximum caffeine levels (40 mM), which also strongly suggests a component of CICR in the caffeine response. This "all or none" response in any given cell has also been observed in isolated mouse myotubes stimulated with 4-chloro-*m*-cresol (Gschwend et al., 1999).

However, myotubes exhibited a typical threshold for CICR, and the number of RyR-expressing 1B5 cells responding increased as the caffeine concentration was increased (Fig. 7 *D*). Given the steepness of the caffeine dose-response curve and possible nonlinearity of the fura 2 dye at caffeine concentrations inducing near-saturating intracellular Ca^{2+}, the threshold response (not the EC_{50}) was a more sensitive measure of the inherent sensitivity of the two RyR isoforms to this activator. For example, the C2C12 cell depicted in Fig. 7 *A* and the RyR1-transduced 1B5 cell in Fig. 7 *B* each had a threshold of 3 mM caffeine. In these cells, regenerative calcium oscillations were elicited with submaximum concentrations of caffeine, whereas at high caffeine concentrations, a sustained calcium increase was observed. In contrast, RyR3-expressing 1B5 cells typically had a lower caffeine threshold, such as the cell shown in Fig. 7 *C* (threshold of 0.3 mM). However, regenerative calcium oscillations were never observed in response to submaximum caffeine concentrations in RyR3-expressing 1B5 cells (also see Fig. 10). Thus two new observations are that although RyR3 has significantly higher sensitivity to caffeine compared with RyR1, only RyR1 can support regenerative oscillations in 1B5 myotubes.

*4-Chloro-*m*-cresol sensitivity*

Both C2C12 cells and RyR1-expressing 1B5 cells responded to CMC (Fig. 8, *A* and *B*). Similar to responses to caffeine, subthreshold concentrations of CMC elicited regenerative calcium oscillations in both cell types. 1B5 cells infected with RyR3-containing viruses exhibited a much lower frequency of responses to CMC compared with RyR1-expressing myotubes (Fig. 8 *C*). Whereas all RyR1-expressing cells that responded to 40 mM caffeine also responded to 100 μM CMC, only 28.8 $\pm$ 3.5% of RyR3-expressing 1B5 cells that responded to caffeine responded to 500 μM CMC (the highest concentration of CMC tested) (Fig. 8 *D*).

To provide a biochemical correlation to differences in sensitivity of RyR1 and RyR3 to RyR agonists, [^{3}H]ryanodine binding analysis was performed on total membrane homogenates isolated from RyR1- or RyR3-expressing 1B5 myotubes under identical assay conditions. When assayed in the presence of 20–50 μM Ca^{2+}, the two receptor isoforms exhibited saturable binding in the range of 1–50 nM [^{3}H]ryanodine and gave similar binding constants. The ap-

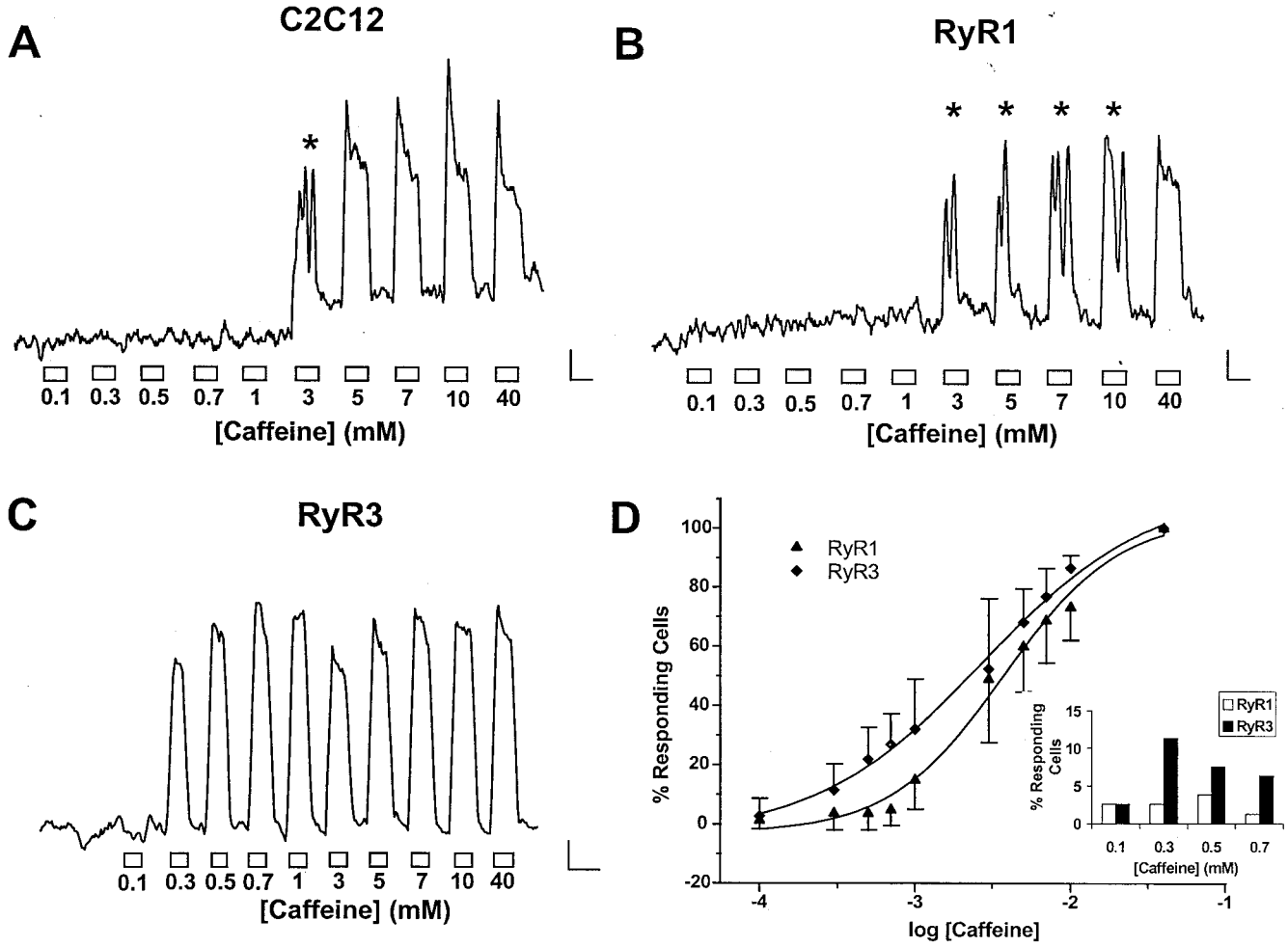

FIGURE 7 RyR1 and RyR3 exhibit different sensitivities to caffeine. Cells were cultured and then imaged for calcium as described in Materials and Methods. Cells were incubated in increasing caffeine concentrations which ranged from 0.1 to 40 mM. Each caffeine incubation period was 60 s; these were separated by 60-s recovery periods. (*A*) Representative trace from a C2C12 cell. Note the presence of calcium oscillations at 3 mM caffeine (*asterisk*). (*B*) Representative trace from a RyR1-expressing 1B5 cell. Calcium oscillations are seen in this cell from 3–10 mM caffeine (*asterisks*). (*C*) Representative trace from a RyR3-expressing 1B5 cell. No calcium oscillations are observed. (*D*) Summary of caffeine dose-response curves obtained from four separate determinations. Responses are normalized to the total number of cells responding to 40 mM caffeine, which is taken to represent the total number of RyR-expressing cells in the field. The number of cells expressing RyR1 and RyR3 analyzed was 67 and 49, respectively. Each point represents a mean ± SD. *Inset*: RyR3 has a lower threshold caffeine concentration required for activation. The percentage of either RyR1- (*open bars*) or RyR3- (*filled bars*) expressing myotubes with a threshold caffeine concentration between 0.1 and 0.7 mM is indicated. Calibration bar: 0.05 340/380 ratio units versus 50 s.

parent higher caffeine sensitivity of RyR3 in intact 1B5 myotubes did not carry over as an increased caffeine sensitivity in [^{3}H]ryanodine binding studies. In these experiments, caffeine enhanced the occupancy of [^{3}H]ryanodine binding to RyR1- and RyR3-expressing membranes in a similar dose-dependent manner (Fig. 9 *A*). The difference in CMC sensitivity between RyR1 and RyR3 was confirmed in [^{3}H]ryanodine binding studies. Fig. 9 *B* shows that although CMC increased the binding of [^{3}H]ryanodine to RyR1 in a dose-dependent manner, saturating at 100% of optimal control (measured in the presence of 100 μM Ca^{2+}), the drug exhibited little efficacy in stimulating ryanodine binding to RyR3.

Calcium waves

Submaximum levels of caffeine or CMC often triggered calcium oscillations in C2C12 cells and RyR1-expressing 1B5 cells. These oscillations originated at a specific region or "trigger zone" in RyR1-expressing 1B5 cells and then propagated as a discrete calcium wave across the cell (Fig. 10 *A*). These oscillations persisted as long as the agonist was present but terminated immediately after the agonist was removed (Fig. 10 *C*). However, suprathreshold levels of caffeine (40 mM; Fig. 10, *B* and *D*) or CMC (500 μM) triggered a global increase in calcium in these cells. In contrast, RyR3-expressing 1B5 cells never displayed cal-

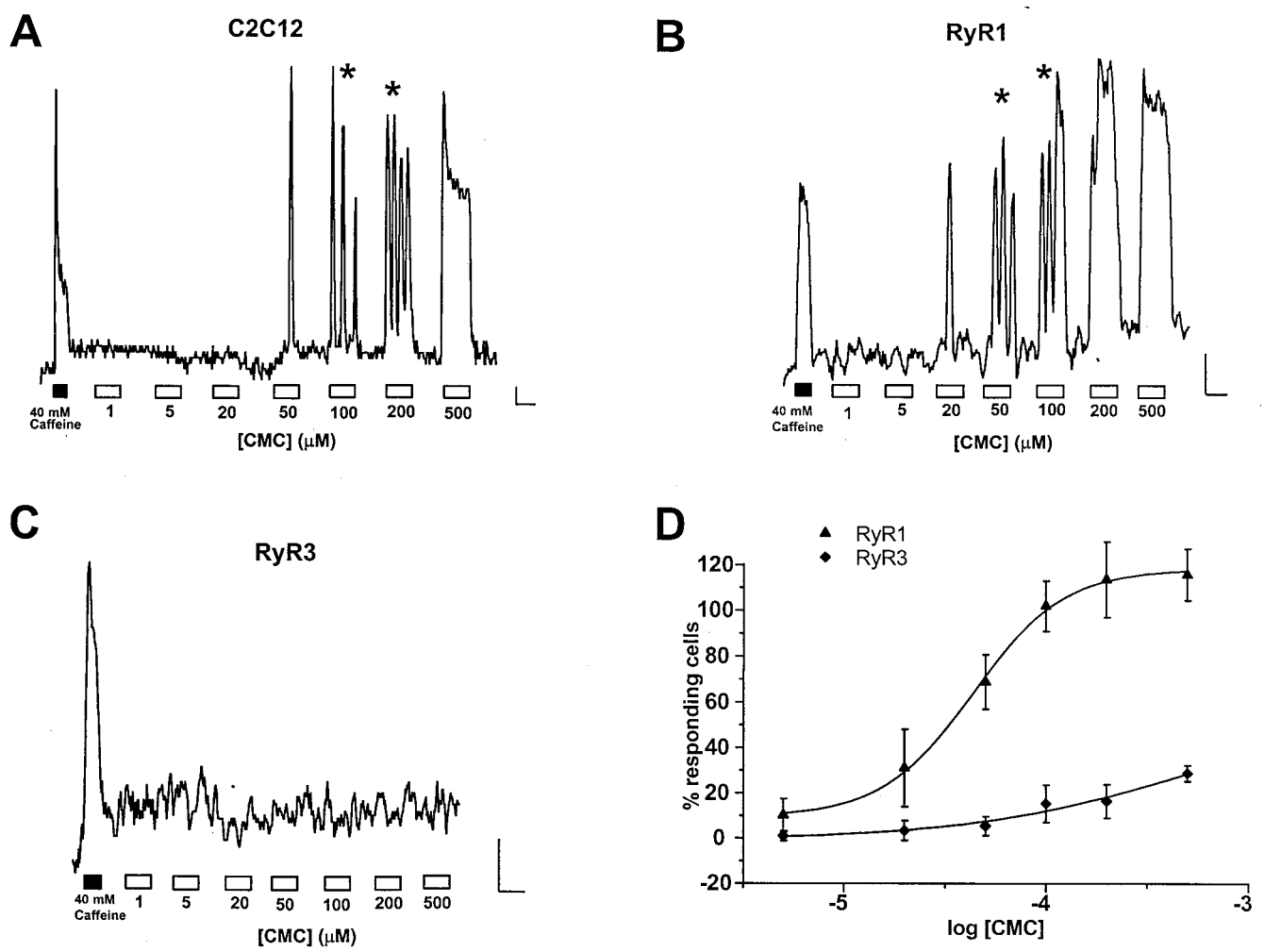

FIGURE 8 RyR1 and RyR3 exhibit differential sensitivity to 4-chloro-*m*-cresol. 1B5 myotubes were cultured and then imaged for calcium as described in Materials and Methods. Cells were first challenged with 40 mM caffeine to determine the number of RyR-expressing cells in the field. Cells were then incubated in increasing CMC concentrations that ranged from 1 to 500 μM. Each CMC incubation period was 60 s; these were separated by 60-s recovery periods. (*A*) Representative trace from a C2C12 cell. Calcium oscillations are observed at 100 and 200 μM CMC (*asterisks*). (*B*) Representative trace from a RyR1-expressing 1B5 cell. Calcium oscillations are observed at 50 and 100 μM CMC (*asterisks*). (*C*) Representative trace from a RyR3-expressing 1B5 cell. No responses to CMC are observed. (*D*) Summary of CMC dose-response curves obtained from four separate determinations. Responses are normalized to the total number of cells responding to the initial application of 40 mM caffeine, which represents the total number of RyR-expressing cells in the field. The number of cells analyzed that expressed RyR1 or RyR3 was 104 and 71, respectively. Each point represents the mean ± SD. Calibration bar = 0.05 340/380 ratio units versus 50 s.

cium oscillations when challenged with any concentration of caffeine. Instead, calcium increases caused by 0.1–4 mM caffeine were observed in small, localized, cellular regions that failed to initiate a calcium wave (Fig. 10 *E*). At higher caffeine concentrations (5–40 mM), global rises in calcium were observed in all 1B5 myotubes expressing RyR3 (Fig. 10, *F* and *G*).

DISCUSSION

The results reported in this study indicate that several functional differences exist between RyR1 and RyR3 expressed in 1B5 myotubes. First, only RyR1 can restore depolarization-induced e-c coupling. Second, there are significant differences in the sensitivity to caffeine and CMC of cells expressing RyR1 and RyR3. Third, the type of calcium release events triggered by caffeine and CMC from these two ryanodine receptors is fundamentally different: RyR1 supports regenerative calcium oscillations in response to submaximum doses of caffeine and CMC, whereas RyR3 does not. Finally, the divergent phenotype of RyR1 and RyR3 appears to be the result of essential protein-protein interactions within the context of a skeletal muscle environment (e-c coupling, Ca^{2+} oscillations, and caffeine sensitivity) as well as fundamental structural differences in drug recognition sites (CMC).

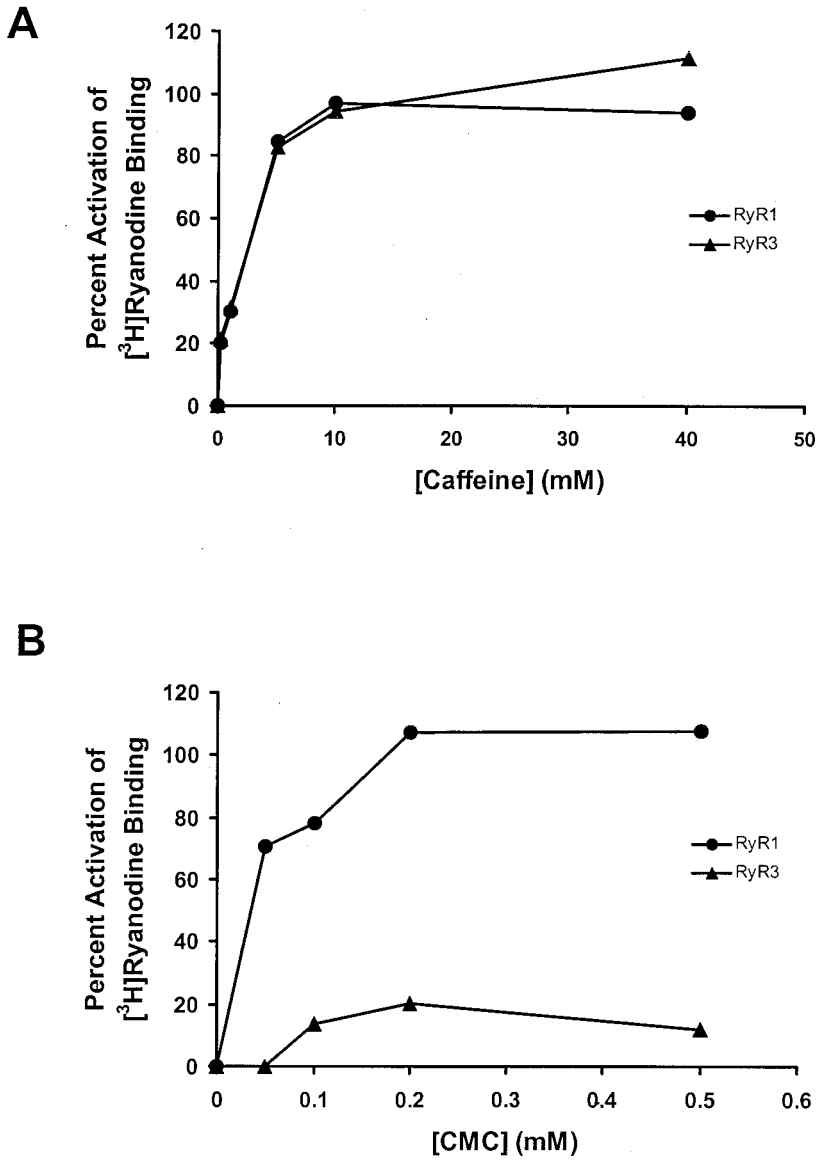

FIGURE 9 Caffeine and 4-chloro-*m*-cresol have divergent effects on [^{3}H]ryanodine binding to RyR1 and RyR3. [^{3}H]Ryanodine binding to microsomal membranes isolated from RyR1- or RyR3-transfected 1B5 cells was measured as described in Materials and Methods. Results represent the average of two determinations, using [^{3}H]ryanodine = 10 nM and [Ca^{2+}]free = 1 μM. Ryanodine binding in these conditions in the absence of RyR agonists was 270 and 89 fmol [^{3}H]ryanodine bound/mg protein for RyR1 and RyR3, respectively, which represents 0% activation on the graph. Results are normalized to the level of ryanodine binding achieved at optimal calcium conditions ([Ca^{2+}]free = 100 μM), which is taken to represent 100% activation. The amount of [^{3}H]ryanodine bound at this optimal calcium level was 890 and 416 fmol [^{3}H]ryanodine bound/mg protein for RyR1 and RyR3, respectively. The effects of increasing levels of caffeine (*A*) or 4-chloro-*m*-cresol (*B*) on [^{3}H]ryanodine binding to RyR1 or RyR3 are indicated.

Expression system

The use of helper-free HSV-1 amplicon virions containing RyR cDNAs (Wang et al., 2000) has greatly enhanced the efficiency of RyR expression in 1B5 myotubes. At the highest level of RyR1 virus tested (2×10^5 IU/ml), 69% of 1B5 myotubes expressed functional RyR1 receptor (as judged by the percentage of infected cells responding to 40 mM caffeine). With increasing virus concentration, we observed a linear increase in the number of RyR1-expressing cells. However, as the number of transduced cells increased, the percentage of RyR1-expressing cells with a "punctate" labeling pattern decreased. As discussed (Protasi et al., 2000), the "punctate" immunolabeling pattern most likely represents the proper targeting of RyR1 to CRUs. This concept is supported by our observation that the recovery of depolarization-induced calcium release was correlated with the percentage of "punctate" immunolabeled cells. Taken together, these findings suggest that proper targeting to CRUs enables RyR1 to couple with the DHPR and restores e-c coupling. That the relative proportion of 1B5 cells containing properly targeted RyR1 decreases as viral titer increases may be due to the increased transduction of less differentiated cells that do not possess the necessary subcellular organization to target RyR1 correctly to the junctions. At lower viral titers, the transduction of well-differentiated multinucleated myotubes is favored, based on their larger size and corresponding larger surface area. This interpretation is also supported by our recent findings obtained with a green fluorescent protein amplicon, which

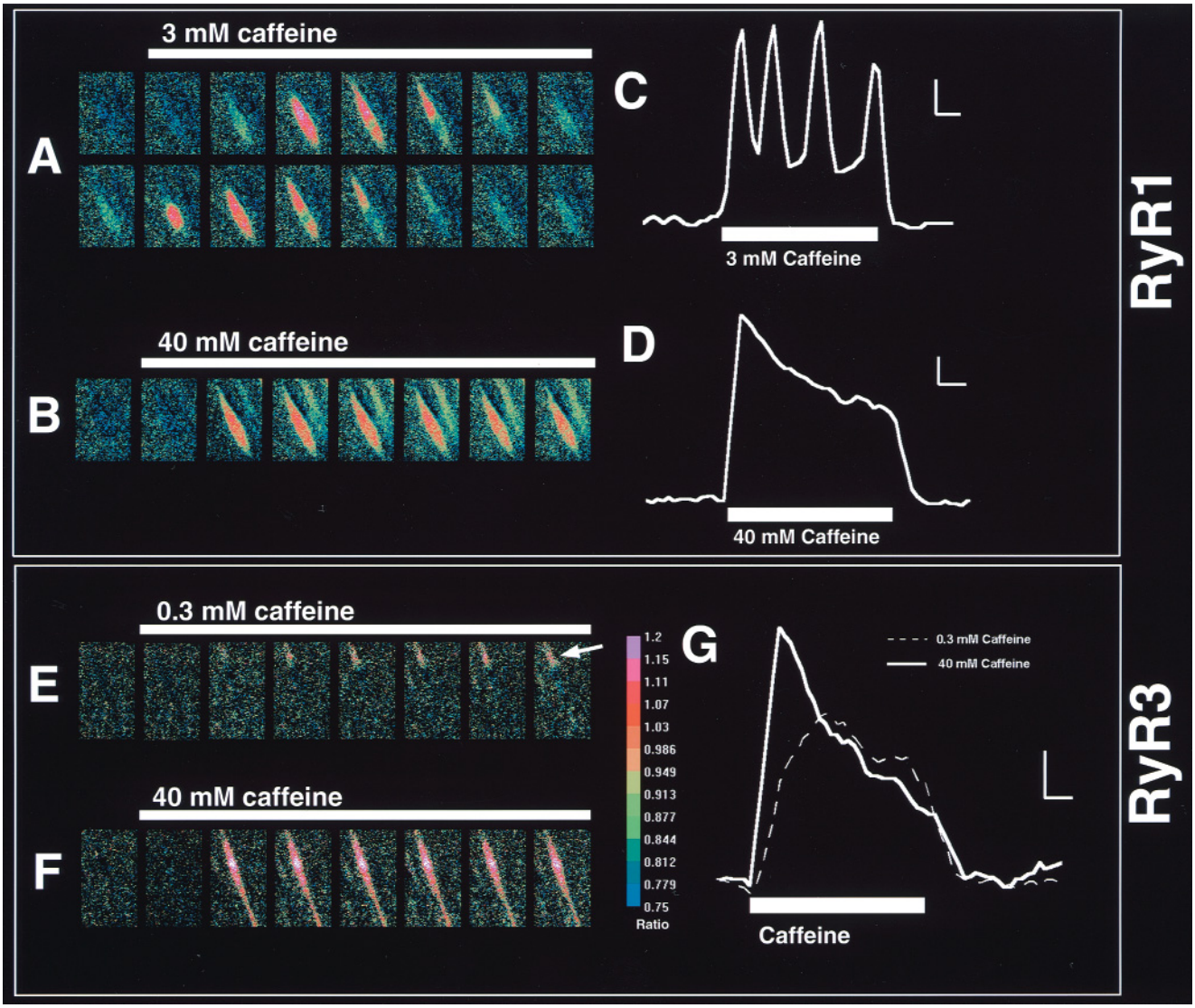

FIGURE 10 RyR1 but not RyR3 supports regenerative calcium oscillations. Cells were cultured and imaged for calcium as described in Materials and Methods. Each panel represents a single F340/F380 ratio image; images are spaced 2 s apart. The calibration bar for these images is indicated at the bottom of the figure. (*A*) Ratio images from a 1B5 myotube expressing RyR1 stimulated with 3 mM caffeine are shown. After 2 s, a calcium wave begins from a discrete region and spreads across the cell. After ~2 s more, the calcium wave occurs again. (*B*) Ratio images from the same cell in *A* stimulated with 40 mM caffeine. (*C*) The corresponding change in the Fura-2 340/380 ratio induced by 3 mM caffeine. (*D*) The corresponding change in the fura-2 340/380 ratio induced by 40 mM caffeine. Calcium increases globally throughout the cell, and no calcium waves or oscillations are observed. Calibration bar for calcium traces: 0.1 340/380 ratio units versus 10 s. (*E*) Ratio images from a 1B5 cell expressing RyR3 stimulated with 0.3 mM caffeine. (*F*) Ratio images from the cell in *E*, simulated with 40 mM caffeine. A larger area of the cell responds, but no calcium waves or oscillations are observed (*G, solid line*). (*G*) A calcium increase is observed in a small discrete region of the cell (*arrow*), but no oscillations are generated, as indicated by the trace (*dashed line*). Calibration bar for calcium traces: 0.05 340/380 ratio units versus 10 s.

revealed more efficient transduction of fully differentiated 1B5 myotubes compared to myoblasts (Wang et al., 2000).

In the present study, functional responses were examined in 1B5 myotubes infected with a viral titer that ensured the highest incidence of "punctate" immunolabeling. Although this approach resulted in a lower than maximum transduction efficiency, it permitted us to have a more direct comparison of functional characteristics exhibited by RyR1 and RyR3 that were properly targeted to junctions and expressed at similar levels.

Heterogeneity of RyR1 functional responses

1B5 cells undergo a series of structural changes during differentiation. Upon withdrawal of serum and an increase in the ambient CO_2 level, 1B5 myoblasts fuse and form elongated multinucleated myotubes. As documented previously (Protasi et al., 1998), a structural reorganization of triadic proteins occurs concomitantly with differentiation, whereby triadin and DHPRs are organized into discrete foci at the cell surface (CRUs). However, the differentiation

process is never complete; i.e., not all 1B5 myoblasts fuse into myotubes with well-defined CRUs. Thus, when differentiated 1B5 cells are infected with RyR-containing virions, both fully and partially differentiated 1B5 cells express RyRs. This concept is important in understanding the functional heterogeneity of RyR-expressing 1B5 cells. We have observed essentially two populations of 1B5 cells expressing RyR1. Of the cells infected at the lower viral titer, approximately 50% of the cells respond to cellular depolarization with skeletal type e-c coupling and to chemical agents that directly activate the RyR1 complex, such as caffeine and CMC. The remaining 50% of the cells respond solely to these direct chemical agonists. There is excellent quantitative agreement between the functional phenotypes reported in the present study and the frequency of cells exhibiting RyRs properly targeted to CRUs reported in the companion paper (table 1 in Protasi et al., 2000). Taken together, these findings strongly suggest that it is the fully differentiated myotubes possessing mature CRUs that exhibit both skeletal e-c coupling and pharmacological responsiveness. Cells that respond only to caffeine and CMC are likely to represent morphologically immature myotubes that lack CRUs.

Excitation-contraction coupling

1B5 cells share similar characteristics with skeletal muscle, such as the ability to differentiate into multinucleated myotubes that form dyadic and triadic junctions between the SR membrane and the cell surface (Protasi et al., 1998). In addition, 1B5 myotubes express key proteins that are present at the junction, including triadin, calsequestrin, FKBP12, the sarco(endo)plasmic calcium ATPase, and DHPR (Moore et al., 1998). Finally, differentiated 1B5 myotubes develop ordered foci or clusters of colocalized DHPR and triadin, which presumably correspond to CRUs (Protasi et al., 1998). Thus these cells contain not only the component proteins necessary for e-c coupling, but also the elegant subcellular organization required for this specialized form of signal transduction.

Upon introduction of the rabbit RyR1 cDNA, depolarization-induced calcium release (e-c coupling) is restored in 1B5 myotubes. Both chemical depolarization (using 40 mM KCl) and electrical field stimulation elicit Ca^{2+} transients in RyR1-transduced 1B5 cells. The relative proportion of cells exhibiting e-c coupling is essentially identical to the number of cells that contain punctate intracellular labeling. These findings strongly suggest that proper targeting of RyR1 to the junctions is necessary for the restoration of e-c coupling by RyR1. The difference in the frequency of responses elicited by K^+ and electrical field stimulation was similar in transduced 1B5 myotubes and C2C12 myotubes and primarily reflects a lack of efficiency in the delivery of field stimulation rather than being related to the structure or function of the CRUs.

Concomitant with this functional restoration of e-c coupling is the ultrastructural localization of RyR1 within 1B5 junctions. As demonstrated (Protasi et al., 2000), RyR1 expression leads to the appearance of feet at SR-plasma membrane junctions, and foci of RyR1 colocalize with DHPR foci in the same cells. In addition, RyR1 expression leads to the formation of well-ordered tetradic arrays of DHPRs with spacing equal to twice the spacing of feet along the SR membrane.

In contrast, RyR3 does not restore e-c coupling in 1B5 myotubes and displays a higher frequency of subconductance transition than does RyR1 when reconstituted in BLM. The divergent phenotype at the cellular level does not stem from improper targeting of the RyR3 protein, because electron micrographs of negatively stained thin sections clearly show that RyR1 and RyR3 are equally capable of targeting to junctions and forming arrays of feet (figure 6 in Protasi et al., 2000) when expressed in 1B5 myotubes at comparable levels. The present findings extend previous work demonstrating a lack of e-c coupling in skeletal muscle isolated from RyR1-deficient mice, where RyR3 is expressed at very low levels (Ivanenko et al., 1995; Takeshima et al., 1995; Nakai et al., 1996). Furthermore, the crooked neck chicken lacks expression of RyRα (equivalent to mammalian RyR1) and e-c coupling despite high levels of RyRβ expression (equivalent to mammalian RyR3; Ivanenko et al., 1995). The most probable explanation for the lack of e-c coupling in RyR3-expressing 1B5 myotubes is that RyR3 cannot form the necessary functional contacts with DHPR. Therefore the DHPR cannot provide orthograde activation of RyR3, nor can it receive retrograde activation from RyR3 to increase calcium influx through the DHPR (Nakai et al., 1996), which could then activate RyR3 via CICR. Complementary evidence for this conclusion exists at the ultrastructural level. As documented by Protasi and co-workers (Protasi et al., 2000), although RyR3 is targeted appropriately to the junctions, it lacks the ability to order DHPR clusters into the tetradic arrays that are seen when RyR1 is expressed. Therefore, a likely explanation for the lack of e-c coupling observed when RyR3 is expressed is that this protein does not or cannot form functional contacts with the α1 subunit of the DHPR and thus membrane depolarization cannot be translated into release of SR calcium. Whether RyR3 participates in normal skeletal muscle e-c coupling via the propagation of the calcium signal generated by RyR1 as has been suggested (Bertocchini et al., 1997) is still a matter of debate.

RyR3 interactions with FKBP12

Another divergence between RyR1 and RyR3 identified in the present study is the higher incidence of subconductance transitions observed with RyR3 reconstituted in BLM, which were especially prominent at suboptimal Ca^{2+} in the *cis* chamber. Using essentially the same RyR3 cDNA con-

struct to transfect HEK293 cells, Chen and co-workers (Chen et al. 1997) did not observe prominent subconductance behavior with purified heterologously expressed RyR3. Furthermore, β-RyR purified from frog muscle by immunoprecipitation also did not appear to exhibit subconductance behavior in BLM studies (Murayama et al. 1997, 1999). One possibility for the divergent behavior of RyR3 in BLM measurements made in the present study is that the protein was improperly targeted to or folded within SR. This is highly unlikely, because electron micrographs of thin sections of 1B5 myotubes expressing RyR1 or RyR3 reveal junctional localization that is essentially indistinguishable (figure 6 in Protasi et al., 2000). Furthermore, other essential elements functionally attributable to RyR3 can be demonstrated at the cellular and single-channel levels (including activation by Ca^{2+} and caffeine, high-affinity binding of [^{3}H]ryanodine, and a predictable failure to recover e-c coupling; see below). A second explanation for the subconductance behavior seen in the present study is the source and nature of RyR3 used in BLM measurements. In this regard, two notable differences from the aforementioned studies are 1) the skeletal muscle context in which mammalian RyR3 was expressed and 2) the fusion of RyR3 within native SR vesicles (as opposed to solubilized purified RyR3). Interestingly, a recent study of RyR3 isolated from bovine diaphragm was deemed to exhibit occasional subconductance transitions, although frequent transitions to the ¼ and ½ levels were conspicuous in the traces provided (Jeyakumar et al., 1998; see Figs. 5 and 7). Therefore the subconductance behavior for mammalian RyR3 expressed within a skeletal muscle context reported here is not a precedent, but is more easily discerned because of the stability of the transitions.

FKBP12, the major T-cell immunophilin, tightly associates with RyR1 with a stoichiometry of four per channel oligomer (Timerman et al., 1993). The present work reveals that heavy SR isolated from 1B5 myotubes possesses significantly higher levels of FKBP12 when RyR1 protein is expressed compared with membranes expressing a similar density of RyR3. These results strongly suggest that RyR3 may have a lower affinity for FKBP12 than does RyR1 and is lost during the isolation of the RyR3-enriched SR fraction by sucrose-gradient sedimentation. Dissociation of FKBP12 from RyR3 during the preparation of SR vesicles may account for the unique subconductance behavior of RyR3 that we observed in single-channel studies. Consistent with this interpretation, the immunosuppressant FK506 dissociates FKBP12 from RyR1, resulting in channels that conduct current with multiple subconductance states (Timerman et al., 1993; Brillantes et al., 1994). Although no direct measures of the relative affinity of FKBP12 or 12.6 for RyR3 are currently found in the literature, the hypothesis that RyR1 and RyR3 may have different affinities for FKBP12 is not unlikely, because RyR1 and RyR2 isoforms are known to differ in their binding interactions with FKBP12 and 12.6 (Barg et al., 1997; Xin et al., 1999).

Responses to caffeine and 4-chloro-*m*-cresol

While the intracellular caffeine dose-response relationship between RyR1 and RyR3 has not been well characterized, several reports have examined the sensitivity of RyR3 to activation by Ca^{2+} at high-affinity cation sites and inhibition by Ca^{2+} and Mg^{2+} at low-affinity sites (Chen et al., 1997; Murayama and Ogawa, 1997; Murayama et al., 1999). Immunopurified RyR3 isolated from diaphragm appears to be less sensitive to activation by extravesicular Ca^{2+} in [^{3}H]ryanodine binding studies than is RyR1. If Ca^{2+} and caffeine sensitivity are controlled through allosteric, mutually interacting sites on the RyR oligomers, one might expect RyR3 to be less sensitive to caffeine. Our results in intact 1B5 myotubes, however, indicate the opposite. Individual myotubes expressing RyR3 have a higher sensitivity to caffeine than RyR1-expressing myotubes, based on the threshold caffeine concentration required to elicit a full cellular response. There are several possible explanations for this observation. First, the affinity for caffeine for its binding site on RyR3 may be greater than it affinity for RyR1, thus giving rise to a lower threshold caffeine concentration required for activation. This possibility is unlikely, however, since, in isolated 1B5 SR preparations, caffeine is equally potent in activating [^{3}H]ryanodine binding of both RyR1 and RyR3. A more likely explanation is that, although the two isoforms have similar affinities for caffeine, the efficacy with which bound caffeine activates the Ca^{2+} release differs. A difference in efficacy observed for caffeine is likely the result of fundamentally different protein-protein interactions between RyR isoforms and accessory proteins at CRUs within the myotube.

Differences in the affinity of RyR1 or RyR3 for the accessory protein FKBP12 may mediate differences in sensitivity to caffeine. In intact skeletal muscle, disruption of the FKBP12/RyR1 complex with FK506 enhances the sensitivity of fibers to depolarization and caffeine (Lamb and Stephenson, 1996; Lamb, 1997). In our model system, the observation of increased caffeine sensitivity in RyR3-expressing 1B5 cells coupled with subconductance behavior of isolated RyR3 channels suggests that an altered interaction between RyR3 and FKBP12 may lead to heightened caffeine sensitivity in intact cells.

Another significant difference between RyR1 and RyR3 is the apparent lack of responsiveness of RyR3 to 4-chloro-*m*-cresol (CMC). CMC activates RyR1 in both isolated skeletal muscle vesicles and intact skeletal muscle (Zorzato et al., 1993; Herrmann-Frank et al., 1996; Tegazzin et al., 1996; Westerblad et al., 1998; Struk and Melzer, 1999), although no reports have assessed the effect of CMC on RyR3. Our results indicate that RyR3-expressing cells are

very insensitive to CMC, and this insensitivity extends to isolated SR, where CMC has negligible effects on [^{3}H]ryanodine binding. This finding represents a large deviation from the potent activating effects of CMC on both RyR1-expressing 1B5 cells and C2C12 cells. Thus the RyR1 protomer may contain a CMC recognition site that either is absent or is of very low affinity in RyR3. Alternatively, RyR1 may interact with an accessory protein that itself binds CMC, but RyR3 may be incapable of this interaction.

Agonist-stimulated cellular calcium responses

At suprathreshold concentrations of caffeine, the spatial aspects of calcium release by RyR1 and RyR3 appeared the same: both isoforms exhibited a sustained global increase in intracellular calcium that resolved after caffeine washout. However, the nature of the calcium responses to submaximum concentrations of caffeine seen in RyR1- and RyR3-expressing cells differed substantially. At submaximum levels of caffeine and CMC, regenerative calcium oscillations were observed in C2C12- and RyR1-expressing 1B5 myotubes, which were similar to caffeine-induced calcium oscillations previously observed in skeletal muscle (Flucher and Andrews, 1993) and C2C12 cells (Lorenzon et al., 1997). On the other hand, in RyR3-transduced cells, submaximum concentrations of caffeine produced small, localized increases in intracellular Ca^{2+} that were not propagated and resolved rapidly.

The different cellular responses of RyR1 and RyR3 to caffeine may be due to the divergent effects of calcium on the two isoforms. Single-channel studies have indicated that micromolar levels of calcium activate RyR3 fully, whereas the same level of calcium can only partially activate RyR1 (Chen et al., 1997; Murayama et al., 1999). In addition, isolated RyR3 channels are much less susceptible to calcium inactivation than are RyR1 channels. When translated to a cellular context, these findings would suggest that when a RyR3 channel is stimulated by caffeine it would be open fully and would tend not to inactivate as readily as RyR1. This activity would discourage calcium oscillations that require repetitive activation and inactivation of the receptor. For RyR1, threshold amounts of caffeine or CMC would partially activate the receptor. As the local calcium level around the channel increased, adjacent RyRs activated by CICR would propagate a calcium wave across the cell, whereas the initiating RyRs would be inactivated by the heightened local calcium concentration. The process would repeat itself because of the continued presence of agonist and the subsequent reactivation of the initiating RyRs. In both RyR1- and RyR3-expressing cells, suprathreshold levels of agonist would activate most RyRs throughout the cell and thus result in a global calcium increase.

In summary, RyR1 and RyR3 expressed in 1B5 myotubes differ in a number of properties, even though these proteins are processed and targeted similarly (see also Protasi et al., 2000). The inability of RyR3 to restore depolarization-induced calcium release provides a functional correlation to its inability to induce DHPR tetrad formation. In addition, RyR3 derived from 1B5 cells has pharmacological properties that are different from those of RyR1 and have not been observed previously. The present results reveal the importance of cellular context when RyR structure function is studied.

We gratefully acknowledge the fine assistance provided by Lili Chen and Dr. Wei Feng in performing single-channel measurements of reconstituted RyR1 and RyR3. We also thank Dr. Gerhard Meissner for kindly providing us with the anti-RyR3 antibody.

This work is supported by National Institutes of Health grants 1RO1AR43140 and 1PO AR1760 and Medical Research Council grant MT-12880 (SRWC).

REFERENCES

Airey, J. A., C. F. Beck, K. Murakami, S. J. Tanksley, T. J. Deerinck, M. H. Ellisman, and J. L. Sutko. 1990. Identification and localization of two triad junctional foot protein isoforms in mature avian fast twitch skeletal muscle. *J. Biol. Chem.* 265:14187–14194 (erratum: *J. Biol. Chem.* 265: 22057).

Barg, S., J. A. Copello, and S. Fleischer. 1997. Different interactions of cardiac and skeletal muscle ryanodine receptors with FK-506 binding protein isoforms. *Am. J. Physiol.* 272:C1726–C1733.

Bertocchini, F., C. E. Ovitt, A. Conti, V. Barone, H. R. Schoeler, R. Bottinelli, C. Reggiani, and V. Sorrentino. 1997. Requirement for the ryanodine receptor type 3 for efficient contraction of neonatal skeletal muscles. *EMBO J.* 16:6956–6963.

Brillantes, A. B., K. Ondrias, A. Scott, E. Kobrinsky, E. Ondriasová, M. C. Moschella, T. Jayaraman, M. Landers, B. E. Ehrlich, and A. R. Marks. 1994. Stabilization of calcium release channel (ryanodine receptor) function by FK506-binding protein. *Cell.* 77:513–523.

Chen, S. R. W., X. Li, K. Ebisawa, and L. Zhang. 1997. Functional characterization of the recombinant type 3 Ca^{2+} release channel (ryanodine receptor) expressed in HEK293 cells. *J. Biol. Chem.* 272: 24234–24246.

Dietze, B., F. Bertocchini, V. Barone, A. Struk, V. Sorrentino, and W. Melzer. 1998. Voltage-controlled Ca^{2+} release in normal and ryanodine receptor type 3 (RyR3)-deficient mouse myotubes. *J. Physiol. (Lond.).* 513:3–9.

Feher, J. J., and M. D. Davis. 1991. Isolation of rat cardiac sarcoplasmic reticulum with improved Ca^{2+} uptake and ryanodine binding. *J. Mol. Cell. Cardiol.* 23:249–258.

Flucher, B. E., and S. B. Andrews. 1993. Characterization of spontaneous and action potential-induced calcium transients in developing myotubes in vitro. *Cell Motil. Cytoskeleton.* 25:143–157.

Flucher, B. E., A. Conti, H. Takeshima, and V. Sorrentino. 1999. Type 3 and type 1 ryanodine receptors are localized in triads of the same mammalian skeletal muscle fibers. *J. Cell Biol.* 146:621–629.

Giannini, G., E. Clementi, R. Ceci, G. Marziali, and V. Sorrentino. 1992. Expression of a ryanodine receptor-Ca^{2+} channel that is regulated by TGF-beta. *Science.* 257:91–94.

Giannini, G., A. Conti, S. Mammarella, M. Scrobogna, and V. Sorrentino. 1995. The ryanodine receptor/calcium channel genes are widely and differentially expressed in murine brain and peripheral tissues. *J. Cell Biol.* 128:893–904.

Gschwend, M. H., R. Ruedel, H. Brinkmeier, S. R. Taylor, and K. J. Foehr. 1999. A transient and a persistent calcium release are induced by chlorocresol in cultivated mouse myotubes. *Pflugers Arch. Eur. J. Physiol.* 438:101–106.

Hakamata, Y., J. Nakai, H. Takeshima, and K. Imoto. 1992. Primary structure and distribution of a novel ryanodine receptor/calcium release channel from rabbit brain. *FEBS Lett.* 312:229–235.

Herrmann-Frank, A., M. Richter, S. Sarkozi, U. Mohr, and F. Lehmann-Horn. 1996. 4-Chloro-*m*-cresol, a potent and specific activator of the skeletal muscle ryanodine receptor. *Biochim. Biophys. Acta.* 1289: 31–40.

Inui, M., A. Saito, and S. Fleischer. 1987. Isolation of the ryanodine receptor from cardiac sarcoplasmic reticulum and identity with the feet structures. *J. Biol. Chem.* 262:15637–15642.

Ivanenko, A., D. D. McKemy, J. L. Kenyon, J. A. Airey, and J. L. Sutko. 1995. Embryonic chicken skeletal muscle cells fail to develop normal excitation-contraction coupling in the absence of the alpha ryanodine receptor. Implications for a two-ryanodine receptor system. *J. Biol. Chem.* 270:4220–4223.

Jeyakumar, L. H., J. A. Copello, A. M. O'Malley, G. M. Wu, R. Grassucci, T. Wagenknecht, and S. Fleischer. 1998. Purification and characterization of ryanodine receptor 3 from mammalian tissue. *J. Biol. Chem.* 273:16011–16020.

Lai, F. A., M. Dent, C. Wickenden, L. Xu, G. Kumari, M. Misra, H. B. Lee, M. Sar, and G. Meissner. 1992a. Expression of cardiac Ca(2+)-release channel isoform in mammalian brain. *Biochem. J.* 288:553–564.

Lai, F. A., Q. Y. Liu, L. Xu, A. el-Hashem, N. R. Kramarcy, R. Sealock, and G. Meissner. 1992b. Amphibian ryanodine receptor isoforms are related to those of mammalian skeletal or cardiac muscle. *Am. J. Physiol.* 263:365–372.

Lamb, G. D. 1997. Ryanodine receptor "adaptation": a flash in the pan? *J. Muscle Res. Cell Motil.* 18:611–616.

Lamb, G. D., and D. G. Stephenson. 1996. Effects of FK506 and rapamycin on excitation-contraction coupling in skeletal muscle fibres of the rat. *J. Physiol (Lond.).* 494:569–576.

Lorenzon, P., A. Giovannelli, D. Ragozzino, F. Eusebi, and F. Ruzzier. 1997. Spontaneous and repetitive calcium transients in C2C12 mouse myotubes during in vitro myogenesis. *Eur. J. Neurosci.* 9:800–808.

Lowry, O. H., N. J. Rosebrough, A. L. Farr, and R. J. Randall. 1951. Protein measurement with the Folin phenol reagent. *J. Biol. Chem.* 193:265–275.

Marks, A. R. 1996. Cellular functions of immunophilins. *Physiol. Rev.* 76:631–649.

McPherson, P. S., and K. P. Campbell. 1993. The ryanodine receptor/Ca^{2+} release channel. *J. Biol. Chem.* 268:13765–13768.

Moore, R. A., H. Nguyen, J. Galceran, I. N. Pessah, and P. D. Allen. 1998. A transgenic myogenic cell line lacking ryanodine receptor protein for homologous expression studies: reconstitution of Ry1R protein and function. *J. Cell Biol.* 140:843–851.

Murayama, T., T. Oba, E. Katayama, H. Oyamada, K. Oguchi, M. Kobayashi, K. Otsuka, and Y. Ogawa. 1999. Further characterization of the type 3 ryanodine receptor (RyR3) purified from rabbit diaphragm. *J. Biol. Chem.* 274:17297–17308.

Murayama, T., and Y. Ogawa. 1997. Characterization of type 3 ryanodine receptor (RyR3) of sarcoplasmic reticulum from rabbit skeletal muscles. *J. Biol. Chem.* 272:24030–24037.

Nakai, J., R. T. Dirksen, H. T. Nguyen, I. N. Pessah, K. G. Beam, and P. D. Allen. 1996. Enhanced dihydropyridine receptor channel activity in the presence of ryanodine receptor. *Nature* 380:72–75.

Olivares, E. B., S. J. Tanksley, J. A. Airey, C. F. Beck, Y. Ouyang, T. J. Deerinck, M. H. Ellisman, and J. L. Sutko. 1991. Nonmammalian vertebrate skeletal muscles express two triad junctional foot protein isoforms. *Biophys. J.* 59:1153–1163.

Pessah, I. N., A. O. Francini, D. J. Scales, A. L. Waterhouse, and J. E. Casida. 1986. Calcium-ryanodine receptor complex: solubilization and partial characterization from skeletal muscle junctional sarcoplasmic reticulum vesicles. *J. Biol. Chem.* 261:8643–8648.

Protasi, F., C. Franzini-Armstrong, and P. D. Allen. 1998. Role of ryanodine receptors in the assembly of calcium release units in skeletal muscle. *J. Cell Biol.* 140:831–842.

Protasi, F., H. Takekura, Y. Wang, S. R. W. Chen, G. Meissner, P. D. Allen, and C. Franzini-Armstrong. 2000. RyR1 and RyR3 have different roles in the assembly of calcium release units of skeletal muscle. *Biophys. J.* 79:000–000.

Saeki, K., I. Obi, N. Ogiku, Y. Hakamata, and T. Matsumoto. 1998. Characterization of brain-type ryanodine receptor permanently expressed in Chinese hamster ovary cells. *Life Sci.* 63:575–588.

Saito, A., S. Seiler, A. Chu, and S. Fleischer. 1984. Preparation and morphology of sarcoplasmic reticulum terminal cisternae from rabbit skeletal muscle. *J. Cell Biol.* 99:875–885.

Sonnleitner, A., A. Conti, F. Bertocchini, H. Schindler, and V. Sorrentino. 1998. Functional properties of the ryanodine receptor type 3 (RyR3) Ca^{2+} release channel. *EMBO J.* 17:2790–2798.

Struk, A., and W. Melzer. 1999. Modification of excitation-contraction coupling by 4-chloro-*m*-cresol in voltage-clamped cut muscle fibers of the frog (*R. pipiens*). *J. Physiol. (Lond.).* 515:221–231.

Takeshima, H., T. Ikemoto, M. Nishi, N. Nishiyama, M. Shimuta, Y. Sugitani, J. Kuno, I. Saito, H. Saito, M. Endo, M. Iino, and T. Noda. 1996. Generation and characterization of mutant mice lacking ryanodine receptor type 3. *J. Biol. Chem.* 271:19649–19652.

Takeshima, H., S. Nishimura, T. Matsumoto, H. Ishida, K. Kangawa, N. Minamino, H. Masuto, M. Ueda, M. Hanaoka, T. Hirose, and S. Numa. 1989. Primary structure and expression from complementary DNA of skeletal muscle ryanodine receptor. *Nature.* 339:439–445.

Takeshima, H., T. Yamazawa, T. Ikemoto, H. Takekura, M. Nishi, T. Noda, and M. Iino. 1995. Ca(2+)-induced Ca^{2+} release in myocytes from dyspedic mice lacking the type-1 ryanodine receptor. *EMBO J.* 14:2999–3006.

Tarroni, P., D. Rossi, A. Conti, and V. Sorrentino. 1997. Expression of the ryanodine receptor type 3 calcium release channel during development and differentiation of mammalian skeletal muscle cells. *J. Biol. Chem.* 272:19808–19813.

Tegazzin, V., E. Scutari, S. Treves, and F. Zorzato. 1996. Chlorocresol, an additive to commercial succinylcholine, induces contracture of human malignant hyperthermia-susceptible muscle via activation of the ryanodine receptor Ca^{2+} channel. *Anesthesiology.* 84:1380–1385.

Timerman, A. P., E. Ogunbumni, E. Freund, G. Widerrecht, A. R. Marks, and S. Fleischer. 1993. The calcium release channel of sarcoplasmic reticulum is modulated by FK-506-binding protein. Dissociation and reconstitution of FKBP-12 to the calcium release channel of skeletal muscle sarcoplasmic reticulum. *J. Biol. Chem.* 268:22992–22999.

Wang, Y., C. Fraefel, F. Protasi, R. A. Moore, J. D. Fessenden, A. DiFrancesco, I. N. Pessah, X. Breakefield, and P. D. Allen. 2000. Helper virus-free HSV-1 amplicon vectors are highly efficient in delivering large genes to skeletal muscle myoblasts and myotubes. *Am. J. Physiol. Cell.* 47:C619.

Westerblad, H., F. H. Andrade, and M. S. Islam. 1998. Effects of ryanodine receptor agonist 4-chloro-*m*-cresol on myoplasmic free Ca^{2+} concentration and force of contraction in mouse skeletal muscle. *Cell Calcium.* 24:105–115.

Xin, H. B., K. Rogers, Y. Qi, T. Kanematsu, and S. Fleischer. 1999. Three amino acid residues determine selective binding of FK506-binding protein 12.6 to the cardiac ryanodine receptor. *J. Biol. Chem.* 274: 15315–15319.

Yaffe, D., and O. Saxel. 1977. Serial passaging and differentiation of myogenic cells isolated from dystrophic mouse muscle. *Nature.* 270: 725–727.

Zorzato, F., E. Scutari, V. Tegazzini, E. Clementi, and S. Treves. 1993. Chlorocresol: an activator of ryanodine receptor-mediated Ca^{2+} release. *Mol. Pharmacol.* 44:1192–1201.